AD-A099 344 UNIVERSITY OF SOUTHERN CALIFORNIA LOS ANGELES ELECTR--ETC F/G 9/5
EVALUATION OF GALLIUM NITRIDE FOR ACTIVE MICROWAVE DEVICES.(U)
MAY 81 M GERSHENZON N00014-75-C-0295

UNCLASSIFIED NL

1 OF 1
AD
A099344

END
DATE
FILMED
6-81
DTIC

LEVEL

FINAL TECHNICAL REPORT

Oct. 1979 - Sept. 1980

EVALUATION OF GALLIUM NITRIDE FOR ACTIVE MICROWAVE DEVICES

Contract Authority: NR 243-004

M. Gershenzon

Electronic Sciences Laboratory
University of Southern California
University Park
Los Angeles, CA 90007

for: Office of Naval Research
Contract N00014-75-C-0295
ONR Code 427
Arlington, VA 22217

AD A099344

DTIC ELECTE MAY 26 1981 C

Approved for public release; distribution unlimited.

Reproduction, in whole or in part, is permitted for any purpose of the U.S. Government.

DTIC FILE COPY

81 5 26 127

SECURITY CLASSIFICATION OF THIS PAGE (When Data Entered)

REPORT DOCUMENTATION PAGE

READ INSTRUCTIONS BEFORE COMPLETING FORM

Field	Entry
1. REPORT NUMBER	243-004 F
2. GOVT ACCESSION NO.	AD-A099344
3. RECIPIENT'S CATALOG NUMBER	
4. TITLE (and Subtitle)	EVALUATION OF GALLIUM NITRIDE FOR ACTIVE MICROWAVE DEVICES
5. TYPE OF REPORT & PERIOD COVERED	Final 1/1/75-9/30/80
6. PERFORMING ORG. REPORT NUMBER	N/A
7. AUTHOR(s)	M. Gershenzon
8. CONTRACT OR GRANT NUMBER(s)	N00014-75-C-0295
9. PERFORMING ORGANIZATION NAME AND ADDRESS	Electronic Sciences Laboratory University of Southern California University Park, Los Angeles, CA 90007
10. PROGRAM ELEMENT, PROJECT, TASK AREA & WORK UNIT NUMBERS	PE 61153N RR021-02-03 NR 243-004
11. CONTROLLING OFFICE NAME AND ADDRESS	Office of Naval Research- Code 427 Arlington, Virginia 22217
12. REPORT DATE	May 81
13. NUMBER OF PAGES	78
14. MONITORING AGENCY NAME & ADDRESS(if different from Controlling Office)	
15. SECURITY CLASS. (of this report)	Unclassified
15a. DECLASSIFICATION/DOWNGRADING SCHEDULE	

16. DISTRIBUTION STATEMENT (of this Report)

Approved for public release; distribution unlimited.

17. DISTRIBUTION STATEMENT (of the abstract entered in Block 20, if different from Report)

18. SUPPLEMENTARY NOTES

Office of Naval Research - Scientific Officer
Telephone Number: (202) 696-4218

19. KEY WORDS (Continue on reverse side if necessary and identify by block number)

Gallium Nitride
Photoluminescence
Saturated Charge Carrier Velocity
Vapor Phase Epitaxy
Crystal Growth

20. ABSTRACT (Continue on reverse side if necessary and identify by block number)

The predicted figure of merit for GaN as a transit-time limited microwave power amplifier material is significantly greater than that of Si or GaAs because of the small electron mass, the large optical phonon energies and the large bandgap of GaN. To confirm these predictions by measuring the saturated drift velocity and the pair-production thresholds, it was necessary to prepare uncompensated n-type single crystals with carrier densities below about 10^{17} cm^{-3}.

DD FORM 1 JAN 73 1473 EDITION OF 1 NOV 65 IS OBSOLETE
S/N 0102-LF-014-6601

SECURITY CLASSIFICATION OF THIS PAGE (When Data Entered)

Because the melting point of GaN is extremely high, > 2,000°C, with a corresponding equilibrium N_2 pressure of > 40,000 atm, it was necessary to use a chemical vapor deposition method (wherein GaCl was allowed to react with NH_3, a more active source of N than N_2 and kinetically stable with respect to N_2 at temperatures below 1100°C) to grow single crystal GaN epitaxially on sapphire substrates. Crystals were grown up to 5 mm in thickness on R-plane oriented substrates. However, their surface morphology was non-planar, and they displayed Ga occlusions, microcracks and voids, the latter two appearing only in the thicker layers. Very slow growth eliminated all these problems except the non-planarity. Epitaxial growth of planar, crystallographically sound crystals was finally achieved on basal plane substrates.

All the crystals grown were n-type with carrier densities of 10^{18} - 10^{20} cm^{-3}. These observed densities were more or less independent of all crystal growth parameters, including replacing the Ga halide reactant source with a Ga organometal source. The distribution of the electrons at these high concentrations was degenerate, so that transport measurements as a function of temperature could provide no information on the nature of the donor or donors responsible.

Such information, however, could be deduced from low temperature, near-gap photoluminescence measurements. Here, bound exciton and donor-acceptor pair transitions specific to individual defects, impurities and dopants were identified and used to characterize as-grown crystals, crystals intentionally doped during growth and samples ion implanted with various chemical species and subsequently annealed.

For shallow levels, the electrical nature of the defect and its ionization energy were uniquely determined. Shallow donors include Si (with a donor ionization energy of 38 meV, Si was always present in the as-grown crystals, dominating the donors and responsible for carrier densities greater than 10^{20} cm^{-3} unless all contact between the reactant gases and the fused silica was avoided in the crystal growth apparatus), Sn (50 meV), Se (15 meV), Ge ($\sim$ 38 meV), and an unknown shallow donor (26 meV) present in the 10^{18} - 10^{19} cm^{-3} range. From these results an electron effective mass of 0.11 m_0 was deduced. The "shallow" acceptors include Cd (201 meV), Ge (203 meV), Be (205 meV), Mg (208 meV), Zn (212 meV) and Li (219 meV). Here an effective mass theory hole mass of 1.3 m_0 was deduced. Using this value for the mass, the shallowest acceptor value predicted is about 200 meV, in agreement with the measured values. This means that even the shallowest acceptor is too deep to generate a significant free hole density at room temperature. Thus, normal high conductivity p-type material, hence p-n junctions are not feasible for GaN at room temperature.

For deep levels, characteristic emission peaks were observed, but ionization energies and even their identity as donor or acceptor could not be deduced in a direct manner. C, O, S and Na are such levels. The first three are probably deep donors, the last, a deep acceptor. H introduces a non-radiative center.

Of all these dopant species, none could be associated with the unknown shallow donor always present in GaN and (after minimizing Si contamination) resulting in the high free carrier density of 10^{18} - 10^{19} cm^{-3} always present in the uncompensated crystals. Chemical analyses of as-grown crystals supported this conclusion. Hence, this shallow-donor must be a native defect. Photoluminescence results on Ga implanted samples and on N implanted samples showed that the former enhanced the presence of this donor, while the latter reduced it. The simplest model for such a defect is an isolated N vacancy.

Although this donor could be compensated, we required uncompensated material of low carrier density. Experiments aimed at eliminating the vacancy,

(Continuation of Abstract)

by annealing or growing under very high pressures of N_2 (8,000 atm) at 1200-1400°C, were not conclusive, because Si was introduced from the high pressure apparatus at levels sufficient to mask the native donor.

Accession For
NTIS GRA&I
DTIC TAB
Unannounced
Justification
By
Distribution/
Availability Codes
Avail and/or
Dist Special
A

TABLE OF CONTENTS

		Page
I.	Introduction	1
II.	Chronology of Progress	4
III.	Thermodynamics	8
IV.	Halide VPE Growth on R-Plane Sapphire	11
V.	Halide VPE Growth on Basal-Plane Sapphire . . .	16
VI.	Organometal VPE Growth	18
VII.	Crystal Growth Parameters and Native Disorder . .	19
VIII.	High Pressure-High Temperature Processing and Synthesis under N_2	21
IX.	Doping and Compensation	24
X.	Transport Properties	28
XI.	Low Temperature Photoluminescence	31
XII.	Bibliography	77
XIII.	Distribution List	78

I. INTRODUCTION

About twelve years ago, with the development and commercialization of LED's and semiconductor lasers, there was a flurry of interest in about a dozen laboratories around the world, including ours, in the wide-band direct gap (3.4 eV), III-V semiconductor GaN, as a possible UV semiconductor laser and as an LED. As an LED, using inexpensive and efficient down-converting phosphors from the UV to the visible, LED's covering the entire visible spectrum might be achieved using a single semiconductor technology, that of GaN. However, it quickly became apparent that GaN was difficult to grow as a single crystal to the exacting specifications of a semiconductor. Of greater significance, was the fact that low resistivity p-type material could not be made. Thus, p-n junctions, the basis of LED's and semiconductor lasers, could not be obtained. Interest in GaN therefore faded, and today there are only two or three research groups in the world still actively pursuing this quest.

Not withstanding these problems, it was realized several years ago that GaN possessed two unique properties eminently desirable in a semiconductor material used as the basis for transit-time-limited (IMPATT, etc.) microwave power amplifiers.

First, the saturated drift velocity should be large leading to short transit times and high frequencies. This follows from the relatively small electron effective mass in GaN, 0.2 m_o, from the large optical phonon energy (120 meV) due to the light mass of nitrogen, and from the fact that the

kinetic energy of a hot electron in GaN is limited primarily by optical phonon scattering. Crudely setting $1/2\ m_e v_s^2 = \hbar\omega_o$, we obtain a saturated drift velocity v_s several times greater than that for either Si or GaAs.

Second, the band gap of GaN is three times that of Si, and more than twice that of GaAs. Pair-production thresholds scale with the band gaps. To avoid continuous avalanche breakdown, the voltage across a reverse biased high field transit-time-limited device must be held at or just below the threshold for pair production. Since this is higher for GaN, such a device would be able to operate at a higher voltage. As a power amplifier the power would scale as the square of the voltage, significantly enhancing the value of GaN over that of Si or GaAs.

These two features (drift velocity and the square of the maximum operating voltage) can be combined into a single material figure of merit for a power transit-time-limited amplifier. This leads to the prediction that GaN as a semiconductor material is at least 20 times better than Si for such devices.

The goal of this contract has been the experimental verification of this conclusion by measuring both the saturated drift velocity and the pair production threshold of GaN, utilizing a Ryder pulsed I-V technique for the former and a photomultiplication study for the latter. Since an IMPATT device is not a minority carrier injection device, p-n junctions are not required; the high field depletion region of a Schottky barrier should suffice. In addition, while working towards the stated goals, we anticipated laying much of the technolo-

gical basis for utilizing GaN as a semiconductor material. As summarized in our previous reports, in order to make these measurements, we require single crystals of n-type GaN with a doping level of less than about $10^{17}/cm^3$ and the material must not be compensated. (Compensation would reduce the low-field mobility.) This then, has been the immediate goal of this contract for the last few years.

In the next section we give a brief summary of the chronology of our efforts under this contract towards achieving this goal. First, we note that we have learned how to grow thick, epitaxial single crystals of GaN that are crystallographically very sound. Second, all acceptors in GaN are relatively deep, so that low resistivity, p-type conduction at room temperature is not possible. Third, a shallow native donor defect is always present and (without compensation) always produces low resistivity n-type material. This donor is now definitively associated with a deficiency of nitrogen, a conclusion only hypothesized until this year.

In the remainder of this report we will describe in detail the crystal growth of GaN, the doping of GaN and the characterization of these crystals, emphasizing our most recent work on the low-temperature photoluminescence characterization of ion-implanted crystals, particularly Ga and N implants.

II. CHRONOLOGY OF PROGRESS

Our initial attempts to grow single crystals of GaN, prior to the start of this Contract, were by liquid phase epitaxy (LPE). This brought us into contact with the first major problem, the thermodynamic constraints on crystal growth of GaN. Like any other III-V compound, GaN might be grown from a melt of its constituents Ga and N_2. However, because the Ga-N bond is very strong, the anticipated melting point is greater than 2000°C, and because the N-N bond in N_2 is very strong, the anticipated equilibrium pressure of N_2 at the melting point is greater than 40,000 atm. (see below). LPE growth on the Ga-rich side of the phase diagram requires a minimum solubility of N_2 of 1% to avoid problems of constitutional supercooling. Typically, this means that the growth temperature should be at least 2/3 that of the maximum melting point. Even at 1,000°C, well below this value, the equilibrium pressure of N_2 is already greater than 100 atm. Thus, without involving high pressure-high temperature equipment, direct LPE growth is not feasible.

Fortunately, it is possible to avoid this difficulty by the use of a non-equilibrium growth reaction involving NH_3, a less stable (more active) source of N than N_2. At 1050°C, 200 atm of N_2 are required to grow GaN. At this temperature and in the presence of 1 atm of H_2, only 5 torr of NH_3 should exist in equilibrium with 100 atm of N_2: $2NH_3 \rightarrow N_2 + 3H_2$. Thus 5 torr of NH_3 are thermodynamically equivalent to 200 atm of N_2. However, below 1100°C, the dissociation of NH_3 into N_2 and H_2 is very slow in the absence of a suitable catalyst.

Hence at 1050°C, GaN growth is possible using a moderate NH_3 pressure which does not equilibrate with N_2 and H_2.

Our original LPE experiment using Ga and NH_3 between 900 and 1100°, showed that the solubility of NH_3 in Ga was far too small at these temperatures to result in GaN crystal growth at reasonable rates. Thus we converted to vapor phase epitaxy (VPE) allowing $\sim$ 100 torr of NH_3 to react with GaCl (generated from HCl and liquid Ga) in an H_2 ambient at about 1050°.

Many substrates were tried. ZnO should provide the best crystallographic match, but it is rapidly etched by the GaCl and HCl. Only sapphire yielded good epitaxy and that became the standard substrate material.

The early VPE crystal growth work done under this Contract yielded single crystal layers, but these were heavily doped n-type, about 10^{20} electrons/cm^3 close to the substrate interface (< 5 μm) and dropping about a factor of 10 for thicker layers. Thus, we desired to grow very thick layers. From experiments on small sapphire spheres, we determined that the most rapid growth of GaN occurred on the pyramidal R-planes. This is also the orientation most easily available. (It is the orientation used for silicon-on-sapphire.) Therefore, we concentrated on growth on this substrate orientation. We learned how to grow GaN single crystals on this orientation up to 5 mm thick on 1 x 2 cm substrates. These crystals were marred, however, by four defects: microcracks, voids, Ga precipitation, and a non-planar, faceted surface. We learned how to eliminate the first three problems, essentially by using a much slower growth rate, but the non-planarity was characteristic of growth on the R-plane.

At this stage, chemical analysis revealed that the high electron concentration was due primarily to Si. By improving the purity of the starting materials, but particularly by inserting an alumina liner in the growth apparatus to avoid contact between the HCl and GaCl with the fused quartz envelope, the Si content dropped two orders of magnitude and the carrier density no longer was a function of layer thickness. Hence, thick crystals were no longer necessary. Therefore, at this stage we switched to growth on basal plane sapphire. The growth rate was slower, avoiding the problems of cracks, voids and precipitation and the surface was truly planar.

However, the grown crystals remained n-type, at $2 - 7 \times 10^{18}$ carriers $/cm^3$. Chemical analyses showed that Si was not responsible, nor was any other impurity clearly implicated, although the limits of analysis did not completely resolve this question. Thus we needed a tool to characterize the defect electronic states present in the crystals. At the high electron densities noted, the crystals were degenerate, so that the temperature dependence of the Hall coefficient yielded no information about the defects.

At this point, we discovered that low temperature (4.2°K) photoluminescence spectra revealed a wealth of information about these defect levels from bound exciton and donor-acceptor pair transitions, providing the best means for characeriziang these defects. Our next effort then was to intentionally dope the crystals with expected shallow donors, shallow acceptors and anticipated impurities naturally occurring during growth. Here we used doping during growth, by subsequent diffusion and, primarily by ion implantation.

Donor and acceptor ionization energies were determined from a Haynes' Rule plot of bound exciton energies. That for donors was established from observed 2-electron bound exciton transitions and from donor-acceptor pair spectra, and that for acceptors was deduced from donor-acceptor pair spectra and from higher temperature free-to-bound transitions. For acceptors (Be, Mg, Zn, Cd, Li) the results show that all acceptors are relatively deep (> 200 meV) in agreement with the anticipated large hole mass in GaN. Thus we encounter the second major problem with GaN (after crystal growth), the fact that low resistivity p-type material at room temperature is not possible. Hence normal p-n junctions are not feasible. For donors, the much lower electron mass ($0.2\ m_o$) allows levels as shallow as 30 meV and most normal donors (Se, Si, Ge, Sn) have energies not much greater than this. However, the shallow donor which dominates the as-grown crystals was not correlated with any of these, nor with any other expected impurity. This past year, in addition to completing the donor and acceptor characterization experiments, we have focussed on the third major problem in GaN, the ubiquitous presence of this shallow donor, and (from ion implantation results) we now show that it cannot be associated with the last impurity on our list of possibilities, H, and that, from Ga and from N ion implants, it is clearly a native defect due to a deficiency of N (or an excess of Ga). In all probability it is a nitrogen vacancy.

III. THERMODYNAMICS

The true (maximum) equilibrium melting point of GaN has never been determined experimentally, but it can be estimated by several methods. First, Van Vechten has calculated the heats and entropies of fusion of all the III-V compounds. From these he estimates melting points. His value for GaN is 2971°C. Second, Madar, et al. measured the solubility of GaN in Ga at 1200° to be 10^{-3}. By scaling this with the equivalent value in GaP and GaAs, we estimate a melting point of 2400°. Third, in the system Ga-N_2, the vapor pressure (almost entirely N_2) in equilibrium with solid GaN and a solution of N_2 in Ga has been calculated by Thurmond and Logan (assuming the entropy of solid GaN is identical with that of the isoelectronic compound ZnO). The vapor pressure over this three-phase system has been measured by Madar to 1150° and very recently by Karpinski to 1550°. Both investigators first pressurize a sample of GaN to a given pressure, then heat to a given temperature and quench. If the sample melts, the pressure was below the equilibrium pressure at that temperature; if it comes through intact, the pressure was greater than the equilibrium pressure. In this way the phase boundary is mapped. Madar went up to 1150°C (3,000 atm); Karpinski to 1550° (20,000 atm). Well below the melting point, a log P vs 1/T plot should be a straight line (yielding the ΔH for the reaction), but as the melting point is approached, the curve must begin bending, because the true melting temperature is a maximum (a minimum in 1/T) on these plots. Scaling these curves to those of GaP and GaAs, from the lack of any observed bending, we estimate that the true melting point must

be greater than 2,000°C (Madar's data) or greater than 2,400° (Karpinski's data). These large values are due to the large strength of the Ga-N bond in GaN. Furthermore, the estimated pressure of N_2 in equilibrium at the melting point must be greater than 40,000 atm from these results. Thus, growth of GaN from a true melt containing equal (or nearly equal) amounts of Ga and N is clearly out of the question.

Furthermore, LPE growth is also quite difficult, since, from Madar's data, the solubility of GaN in Ga at 1200° is only 10^{-3}. This is too low for conventional LPE growth and here the equilibrium N_2 pressure is already 2,000 (Karpinski) or 5,000 atm (Madar).

Thus we turn to the non-equilibrium use of NH_3 instead of N_2 as the source of nitrogen. Above 1100°, NH_3 equilibrates rapidly to N_2 and H_2. Below 1100°, the homogeneous reaction kinetics are slow. At 1050° the equilibrium pressure of N_2 over GaN is 150 atm (Thurmond) or 300 atm (Madar). At 1050°, with 1 atm of H_2, about 5 torr of NH_3 should be in equilibrium with 200 atm of N_2 (JANAF Tables). Thus, 5 torr of NH_3 are now equivalent to 200 atm of N_2, and GaN can be grown from Ga and NH_3 (instead of from Ga and N_2) at reasonable pressures.

Note that GaN itself is a catalyst for the equilibration of NH_3 and N_2. At 1050° the equilibrium pressure of N_2 over GaN should be 200 atm of N_2. Below this value, the surface of the GaN decomposes producing N_2 and Ga. However in the presence of more than 5 torr of NH_3 the Ga produced on the surface quickly reforms GaN. Thus the net effect of the GaN is to catalyze the conversion of NH_3 to N_2.

As noted earlier, the solubility of NH_3 in Ga at 1050° from a 5 torr gas phase is too small to allow normal growth rates for LPE growth. Therefore we used VPE growth, introducing the Ga as GaCl in the presence of NH_3 at a pressure greater than 5 torr.

IV. HALIDE VPE GROWTH ON R-PLANE SAPPHIRE

As noted earlier, it was desirable to grow very thick crystals in order to reduce the effect of the interface on the observed carrier density (later shown to be associated with Si contamination), and preliminary experiments showed that growth was most rapid on the R-plane orientation $(01\bar{1}2)$ of sapphire. Thus, an open-tube, chemical vapor deposition reactor (Fig. 1) was set up to generate GaCl from HCl gas and liquid Ga and react this with NH_3 in the presence of an R-plane sapphire substrate. The reactor and the growth conditions are described in detail in our previous reports. Briefly, the reactor consists of a fused silica tube containing a concentric alumina liner to avoid generation of Si from the fused silica envelope. HCl in a H_2 carrier enters from one end and passes over two boats containing Ga at 950°. The two boats provide a large enough surface area to completely convert the HCl to GaCl. This flows up a thermal gradient to a long flat zone at 1050° where the NH_3 (in H_2) is injected from a concentric inlet tube. 1050° is high enough to allow rapid growth kinetics, yet low enough so that the NH_3 does not equilibrate to N_2 and H_2. On mixing, the NH_3 is present in excess ($\sim$ 200 torr) of the pressure required to initiate growth ($\sim$ 5 torr). The mixture is very supersaturated and growth of GaN occurs preferentially on the substrate placed close to the tip of the NH_3 inlet. The substrate is placed on a tilted alumina holder which allows maximum contact between the newly mixed flowing gases and the substrate. (Sometimes a second substrate is placed downstream, although growth on this sub-

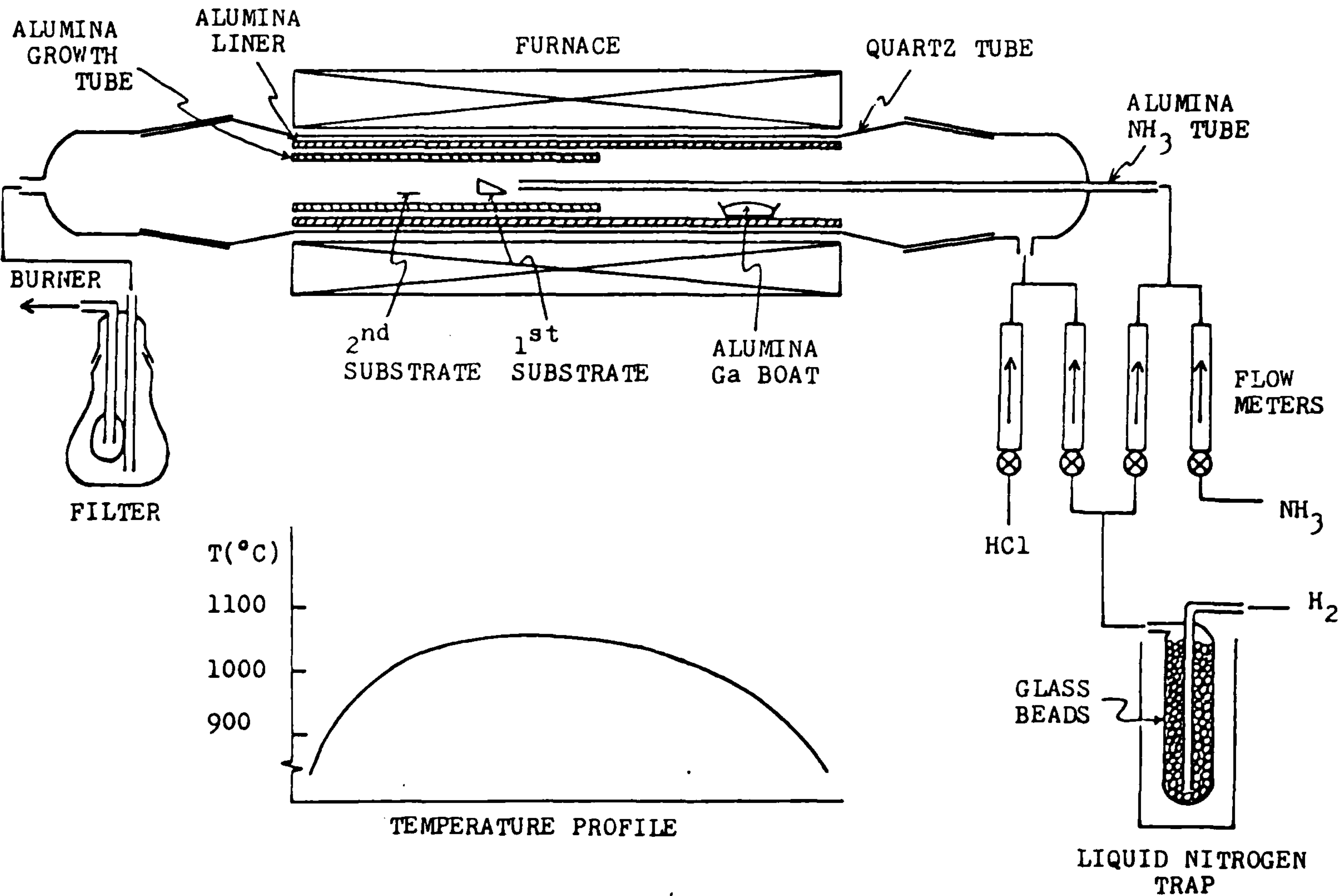

Schematic diagram of open-tube CVD system for growing GaN

Fig. 1

strate is slower due to the large relief of supersaturation by growth already having occurred on the first substrate. Under these conditions of excess NH_3, the growth rate is proportional to the GaCl flow rate; hence it is completely controlled by the injection rate of the HCl.

After the flow rates and temperatures were optimized, the typical growth rate was 15-30 μm/hr. Single crystal layers as thick as 3 mm were grown on 1 x 2 cm substrates. The GaN grows with a $(11\bar{2}0)$ prism plane parallel to the R-plane substrate. The c-axis is in this plane. This is the best lattice match between GaN and R-plane sapphire.

The initial growth consists of island nucleation. The islands are dominated by $(01\bar{1}0)$ prism planes, edged with $(01\bar{1}1)$ and $(10\bar{1}1)$ pyramidal planes. As the islands grow, they merge at a thickness of about 1 μm and the prism planes then disappear from prominence as the coherent crystal continues to grow, leaving the pyramidal planes to form facets on the growing surface. Thus, the first problem emerges: growth is not planar.

At thicknesses greater than 100 μm several other pyramidal planes begin to appear. These are the $(\bar{1}011)$ and $(0\bar{1}11)$ planes and they are retrograde planes leading to re-entrant edges. In addition, large prism plane facets develop from the edges of the substrate, eventually enclosing almost the entire crystal at thicknesses greater than 1 mm. The re-entrant edges lead to the development of retrograde terraces, cave-like structures. Presumably, reactant gas entry and expended gas exit from these regions is restricted, so that very often small voids develop around these caves. This is the second problem in growth.

It can be minimized by slowing the growth rate to 1-10 μm/hr. Now, presumably, the stagnant gases in the caves can be replenished before the growing crystal seals off the cave.

The third problem to face us was the appearance of precipitated Ga particles. These particles are < 100 Å in size, but in sufficient concentration they scatter enough visible light to render the crystals opaque. They are not random in nature, but occur in meandering planes which decorate the growing surface in time. Thus, they are caused by some periodic growth instability in time. Attempts to alter the growth conditions and flow geometry had little or no effect. However, slowing the growth rate to 1-10 μm/hr eliminated this problem as well.

The fourth problem was the appearance of microcracks in the GaN. These appeared only when the layers were thicker than 200 μm. These cracks start from the outer surface of the GaN, not from the GaN-sapphire interface. They are due to the fact that sapphire has a larger coefficient of thermal expansion than GaN. During furnace cool-down after growth, the sapphire shrinks faster than the GaN. Hence, at the interface the sapphire is in tension, the GaN in compression and the sapphire is often cracked. However for thick GaN layers, bending moments result. The GaN surface beomes convex and the outer surface goes into tension and cracking can occur from this surface. This problem, which appears only for layers thicker than 200 μm, can be avoided by stopping crystal growth at a thickness less than 200 μm, grinding the constraining substrate completely off, then continuing growth beyond 200 μm.

Crystals which are grown at slow growth rates, 1-10 μm/hr, and which are less than 200μm thick, are structurally very good single crystals. The only defects observable in thinned samples by transmission electron microscopy are occasional stacking faults and dislocations. However, the surface is not planar, and of course, they are always n-type with 10^{18} - 10^{19} carriers/ cm^3.

V. HALIDE VPE GROWTH ON BASAL-PLANE SAPPHIRE

When it was realized that very thick crystals were no longer required after the Si contamination problem was solved, and noting that the original substrate orientation experiments indicated that while growth on basal plane sapphire was not as rapid as that on R-plane sapphire, the growth however appeared to be planar, it was decided to shift to basal plane substrates, even though these are three times as costly as R-plane substrates. This process involved a complete repetition of the growth optimization procedures. It is described in our report of two years ago. The substrate preparation method required alteration and the flow rate parameters and the positioning of the substrate were changed, but the growth temperature, 1050°C, remained as before. The initial growth stages here also involve island nucleation, but the interface energy is apparently smaller, so that high supersaturation of the reactants leads to polycrystalline nucleation. Thus it was important to reduce the supersaturation, at least during the nucleation phase. In addition, a very high NH_3 pressure (250 torr) had to be used to produce a large density of nuclei, which then grew laterally and merged before they were very high (well below the 1 μm height characteristic of growth on the R-plane). Because of this low interface energy, poisoning of the substrate surface by impurities was very critical, and so the substrate cleaning and handling techniques had to be carefully controlled.

Once these techniques were mastered, crystals could be grown at rates between 30 and 60 μm/hr, faster than on R-plane substrates. The layers, typically, were 30 μm thick and are crystallographically sound single crystals of good optical quality. They do not exhibit the voids and Ga precipitation found in rapidly grown R-plane material, and since they are less than 200 μm thick, no microcracks appear. But their outstanding feature is that they are planar with perhaps a few small ($\sim$ 1μm) steps. The inherent, background shallow donor density, however, appears to be somewhat larger than on R-plane substrates, 1-8 x $10^{19}/cm^3$ here, compared with 2-7 x $10^{18}/cm^3$ on R-plane sapphire with the lower values corresponding to the faster growth rates.

VI. ORGANOMETAL VPE GROWTH

In order to ascertain whether the high densities of the shallow native donor were somehow associated with the halide VPE growth technique, we grew a layer of GaN on R-plane sapphire several years ago by reacting $(CH_3)_3Ga$ with NH_3 at 1050°. The layer was not planar and its resistivity indicated an electron density of $\sim 10^{19}/cm^3$ in the same range as for the halide growth technique. More recently, we have grown GaN on basal-plane sapphire by the same reaction, but at temperatures as low as 900°. These layers are planar, but they are still characterized by a native shallow donor concentration of $\sim 10^{19}/cm^3$. (This work is being done under another contract aimed at producing $Al_xGa_{1-x}N$ alloys for UV photovoltaic applications.) Thus, the high density of native donor defects is not associated with the specific peculiarities of the halide VPE growth technique.

VII. CRYSTAL GROWTH PARAMETERS AND NATIVE DISORDER

Since the true melting point of GaN is greater than 2,000°C, with the equilibrium N_2 pressure greater than 40,000 atm, growth at a temperature of 1050°C is clearly on the Ga-rich side of the phase diagram, even though our growth method is not LPE, but VPE, and even though NH_3 is used instead of N_2. GaN is a fairly ionic semiconductor--its structure is wurtzite not zincblende, and its band gap is large. Thus, we expect a large Schottky native disorder constant. Hence, under the Ga-rich conditions of growth, we expect large deviations from stoichiometry in the direction of an excess of Ga or a deficiency of N, i.e., in simplest form, either Ga interstitials or N vacancies. It is assumed that the ever-present shallow native donor is one of these species, and later we will show from photoluminescence characterization of samples ion implanted with Ga and with N that the native donor density is influenced by such treatment, with the N implants reducing the native donor concentration as expected.

It has already been noted that after the possibilities of Si contamination were removed, standard halide VPE growth on basal plane sapphire led to GaN layers more heavily doped with the native donor ($1\text{-}5 \times 10^{19}/cm^3$) than in layers grown on R-plane sapphire ($2\text{-}7 \times 10^{18}/cm^3$), and that more rapid growth rates favored the lower ends of these ranges. Presumably, it is the kinetically established ratio of Ga to N-containing species on the surface of the growing crystals that determine these densities. The NH_3 pressure, one of the

optimized growth parameters, is about 100 times greater than that necessary to prevent decomposition of GaN at 1050°. This is true both for growth on R-plane and on basal-plane sapphire. Under these conditions, growth should be linear in GaCl pressure, or in the flow rate of HCl over the Ga boats. This is in fact, observed. The growth rate does not vary as the NH_3 flow rate is varied over a wide range, but it does vary linearly with the HCl flow rate. Under such circumstances, it is assumed that the surface of the growing crystal is saturated with the N-containing species. We then measured the growth rate as a function of NH_3 pressure, holding the HCl flow rate fixed on R-plane substrates, it was found that the growth rate did begin to depend on NH_3 pressure at low pressures. It became non-linear in GaCl pressure, when the NH_3 pressure was below about 20 torr (about 10 times the stability pressure). Here, it is expected that the growing surface is no longer saturated with N. Hence the crystal grows under a lower N activity and the native donor density should increase. Under such conditions, growth rates are slow, but several thin samples (1-5 μm) were grown. However, from photoluminescence measurements, the native donor density did not increase. Therefore, all we can conclude is that we do not understand the kinetics at the growing interface.

VIII. HIGH PRESSURE-HIGH TEMPERATURE PROCESSING AND SYNTHESIS UNDER N_2

By this time it has become clear, that the GaN grown by our standard, optimized VPE method from GaCl and NH_3 is dominated by a native shallow-donor corresponding to Ga-rich conditions, probably a N vacancy. Compensation with an acceptor could reduce the electron concentration to a level suitable for the desired drift velocity measurements, but compensation would degrade the low-field mobility, requiring a much higher electric field to attain saturated velocity and resulting in a non-acceptable value of power dissipation to perform this measurement. Thus the native donor must be eliminated, not compensated. This means growing or equilibrating at higher equivalent nitrogen pressures. In the last section we showed that at the optimized growth conditions, the growth rate and the native donor density no longer depended on the NH_3 pressure. The nitrogen species on the growing surface (N, NH, NH_2, ?) was saturated and could not be increased by increasing the NH_3 pressure. Hence the native donor density could not be reduced. The growth temperature, 1050°C, is far below the maximum melting point, > 2,000°C, so that bulk diffusion is very slow. Thus, it was desirable to grow or equilibrate crystals at higher temperatures, above 1100°, where NH_3 is no longer kinetically stable, and at much higher equivalent nitrogen pressures. This meant processing at temperatures above 1100°C, and in an ambient of N_2 at pressures greater than 400 atm.

A high pressure-high temperature system was assembled consisting of two gas compressors, one capable of achieving 3,000 atm, the other, 14,000 atm. Three heated high pressure vessels were coupled to these compressors. One was an externally heated autoclave, rated to 4,000 atm at 1100°. The other two were internally heated vessels, capable of operating up to 1400° at a pressure of 10,000 atm. Fortunately, N_2 is relatively non-reactive and can be used directly in these systems.

In the first experiments, in the externally heated vessel, GaN crystals were equilibrated with N_2 at temperatures between 800 and 1030°C and at N_2 pressures to 3,000 atm. No change in electron density was detected, but some surface decomposition occurred, presumably by transport of Ga as Ga_2O due to the presence of small amounts of O_2 and H_2O as contaminants. By cleaning up the system and gas supply with a small amount of added H_2 and using cold traps we were able to stop the decomposition, but with no effect on the carrier density. These results were extended to 1200° and 9,000 atm in one of the internally heated vessels.

GaN was then grown from Ga and N_2 by LPE in one of the internally heated vessels at temperatures to 1200°C and N_2 pressures to 8,600 atm. R-plane sapphire substrates were submerged in the Ga. The experiments consisted of first pressurizing the vessel with N_2 to 8,600 atm, then heating to 1200°, quenching, then depressurizing. Two forms of GaN were grown. First, on the surface of the Ga liquid, a thin microcrystalline crust formed. This was of high resistivity, perhaps due to the grain boundaries. Second, multiple island

nuclei of GaN formed on the R-plane substrate. These were of typical low resistivity ($\sim 10^{-3}$ ohm cm). However, photoluminescence showed that the dominant donor was Si, not the native shallow donor. As attempts were being made to reduce the Si contamination level in the system, our funding was reduced forcing us to abandon these high-pressure, high-temperature experiments.

Simultaneous with these experiments, a research group in France, led by Madar and Jacob, used similar equipment to map part of the GaN-Ga-N_2 phase diagram, as noted earlier. Crystals that they grew were also low resistivity n-type, as were ours. Very recently (still unpublished), Karpinski, et al. in Poland have extended the phase diagram data to 20,000 atm and temperatures to 1600°C. All the crystals that they produced were high resistivity. It is not clear whether these are compensated or whether they are inherently free of the native donor. However, since they observe high resistivity at the low end of the temperature-pressure range, overlapping our range and that of Madar and Jacob, we must conclude that all of their samples are contaminated with a compensating acceptor.

IX. DOPING AND COMPENSATION

Diffusion by a substitutional mechanism is normally extremely slow unless the temperature of the material is at least 2/3 - 3/4 of the melting point. Since the maximum melting point of GaN is greater than 2000° and the highest temperature at which GaN can be processed is only about 1100° under NH_3, introduction of donors or acceptors by diffusion cannot be a viable process. We have had no success in incorporating several possible compensating impurities. Even Zn, which should diffuse by an interstitial mechanism at even lower temperatures could not be detected near the surface by photoluminescence. Here we must note that at 1000-1100°, under NH_3, the surface is being continuously regenerated. GaN decomposes to form Ga liquid and N_2 and the Ga then reacts with NH_3 to reform GaN. Thus, the effective surface concentration of the Zn may be determined by its solubility in Ga, rather than on some surface state on GaN. In addition, small amounts of O_2 or H_2O can erode GaN by converting the cation to the vapor species Ga_2O. If this erosion is more rapid than the diffusion process, clearly the impurity will never penetrate the solid. We have even tried Li. Li should be an interstitial donor, but it should have the highest (interstitial) diffusion constant of any element (with the exception perhaps, of atomic H). Even here, we could not detect Li in the bulk of a diffused sample by photoluminescence or by a change in the bulk resistivity. In thick R-plane crystals which exhibitted microcracks, the Li quickly migrated down the cracks, decorated them with a precipitated Li-containing species.

Doping during growth is also not easy. Pankove (RCA) and Madar and Jacob (France) attempted to prepare p-n junctions in GaN by doping with Zn during growth. Here a separate controlled hot zone is required to vaporize the Zn. Because of the depth of the Zn acceptor, 200 meV (see below) low resistivity, p-type material could not be obtained. But the Zn should compensate the native donor, leading to high resistivity material. However, the Zn incorporation mechanism appears complex, depending on excess HCl pressure as well as on Zn pressure. Apparently in the initial stages of doping the material continues growing low resistivity n-type. Only after some time, does the resistivity go up, as though a certain amount of Zn has first to be used to tie up some unknown chemical species before it can enter the growing crystal as a simple compensating acceptor. In the latter stages of growth under Zn it is not known whether the Fermi energy has moved down close to the Zn acceptor level or whether it is much closer to the conduction band. Thus, simple p-n junction LED's, the original goal of both these investigators, could not be realized. Instead, MIS structures were fabricated by depositing a metal on the high resistivity, Zn-doped I layer. With high fields across the I layer, minority carriers were generated, leading to radiative recombination in the visible.

We have tried to compensate GaN during growth by two different techniques. First, from photoluminescence measurements (see below) we know that Ge behaves amphoterically as both a donor and an acceptor. Thermodynamically, in the presence of the high native donor density, one would expect the acceptor solubility to be enhanced relative to that of the donor. Thus

we used a GeH_4 dopant stream during growth to introduce Ge. Because GeH_4 cracks to Ge at temperatures as low as 200°C, HCl had to be added to the gas stream to carry the Ge to the hot growth zone as a halide species. Although this method has the ability to control the compensating acceptor simply by controlling the GeH_4 flow, we could not achieve any significant degree of compensation, although photoluminescence showed that Ge was being incorporated in the grown crystal, but both as a donor and as an acceptor simultaneously. We do not know whether the native donor density increased, but the net carrier density remained about the same.

Our second approach towards compensation during growth was to use C. From photoluminescence, we know that C produces only one level and it is deep, too deep to determine if it is a donor or an acceptor. From its position in the Periodic Table adjoining N, we assumed that its solubility on an anion site would be higher than on a Ga site. This is true for GaP and for GaAs. Thus, we guessed that C would act as a deep acceptor. C is easily introduced in the gas stream as CH_4. With CH_4 pressures as high as 10^{-2} atm, where C particle precipitation in the grown crystals becomes evident, the electron density increased (up to $1 \times 10^{20}/cm^3$), and compensation did not occur. Again, our intuitive notions failed.

Our third approach towards doping was by ion implantation. This was our most successful technique, largely because it matched our analysis technique, photoluminescence, rather well. All our GaN samples contain $\sim 10^{19}/cm^3$ of the shallow native donor. Because of the relatively small electron effective mass (0.2 m_o) in GaN, such samples are always degenerate at

room temperature. Hence Hall effect data vs. temperature, due to the absence of carrier freeze-out, provide no information about the identity of the donors or acceptors contributing to the free carrier concentration. However, as described below, low temperature photoluminescence reveals a variety of peaks, mostly bound exciton transitions, each of which is characteristic of a specific donor or acceptor impurity. This technique became our standard analytical tool for determining ionization energies and estimating concentrations of the dopant impurities. The nitrogen laser used to excite the luminescence has a penetration depth of about 2,000 Å in GaN. This is well within the penetration depths of ion implanted species. Thus, the energies of the incident ions were chosen via LSS theory to yield implant depths slightly larger than this value and the total implant dosages were chosen to generate densities from 5×10^{17} to $5 \times 10^{19}/cm^3$ within this depth.

Before implantation, all samples contain the native shallow donor, and, often, the Si donor, both of which are measured in photoluminescence. After implantation with any ion, these peaks are greatly attenuated, presumably due to radiation damage which produces non-radiative recombination sites. From a study of photoluminescence following isochronal annealing experiments of Ar implanted samples, it was found that 3 hours at 1000°C in a flowing NH_3 atmosphere (1 hour is almost sufficient) rejuvenated the native donor and Si photoluminescence peaks to their former strength. Thus the annealing procedure was established.

The implanted ion species included Si, Ge, Sn, S, Se, Zn, Cd, Be, Mg, C, O, Li, Na and H as well as Ga and N. Their characterization from photoluminescence data will be described below.

X. TRANSPORT PROPERTIES

Hall Effect and resistivity measurements vs. temperature on bulk crystals have been described in previous reports. With electron concentrations in these bulk samples always greater than 1 x $10^{18}/cm^3$, the carrier distribution is degenerate, freeze-out does not occur, and, therefore, ionization energies and compensation levels cannot be deduced. (This type of information was obtained from the low temperature photoluminescence, data described in the next section.) The ion-implanted samples may have been compensated to carrier densities below the degeneracy limit, but these were in very thin (2000-3000 Å) layers on n-type very low resistivity crystals and 4-point probe resistivity and van der Pauw Hall measurements yielded results characteristic of the substrate, since the current paths were predominantly in the heavily doped substrate. However, in samples implanted with acceptors, it was often difficult to make ohmic contact, indicating that these layers were significantly compensated. Schottky barriers to the heavily n-type crystals were always ohmic in nature, presumably due to the ease of tunneling through the very narrow depletion regions caused by the high doping levels. Thus, C-V profiling was not possible. (No attempts were made in this study to fabricate Schottky barriers on top of the thin ion-implanted layers.) Thus, the only transport data obtained were on the thick, as-grown, heavily doped crystals.

It has already been noted that the early samples, contaminated with Si, indicated carrier densities up to $10^{21}/cm^3$. Growth on R-plane sapphire yielded samples containing 2-7 x $10^{18}/cm^3$ of the native shallow donor defect, while those grown on basal plane substrates exhibitted a density of 1-6 x $10^{19}/cm^3$, with rapid growth favoring the lower end of the range. It was noted further that the $GaCl/NH_3$ ratio during growth was not a factor.

The latest compilation of mobility vs. carrier density data, as measured at room temperature on bulk samples is shown in Fig. 2. These are all uncompensated crystals, so that the carrier concentration equals the shallow donor concentration and equals the total ionized impurity concentration. Here the ionized impurity concentration is always great enough, so that it alone determines the mobility. Estimates of the room temperature intrinsic mobility, determined primarily by polar optical phonon scattering and by piezoelectric scattering range from 400 to 600 cm^2/V-sec.

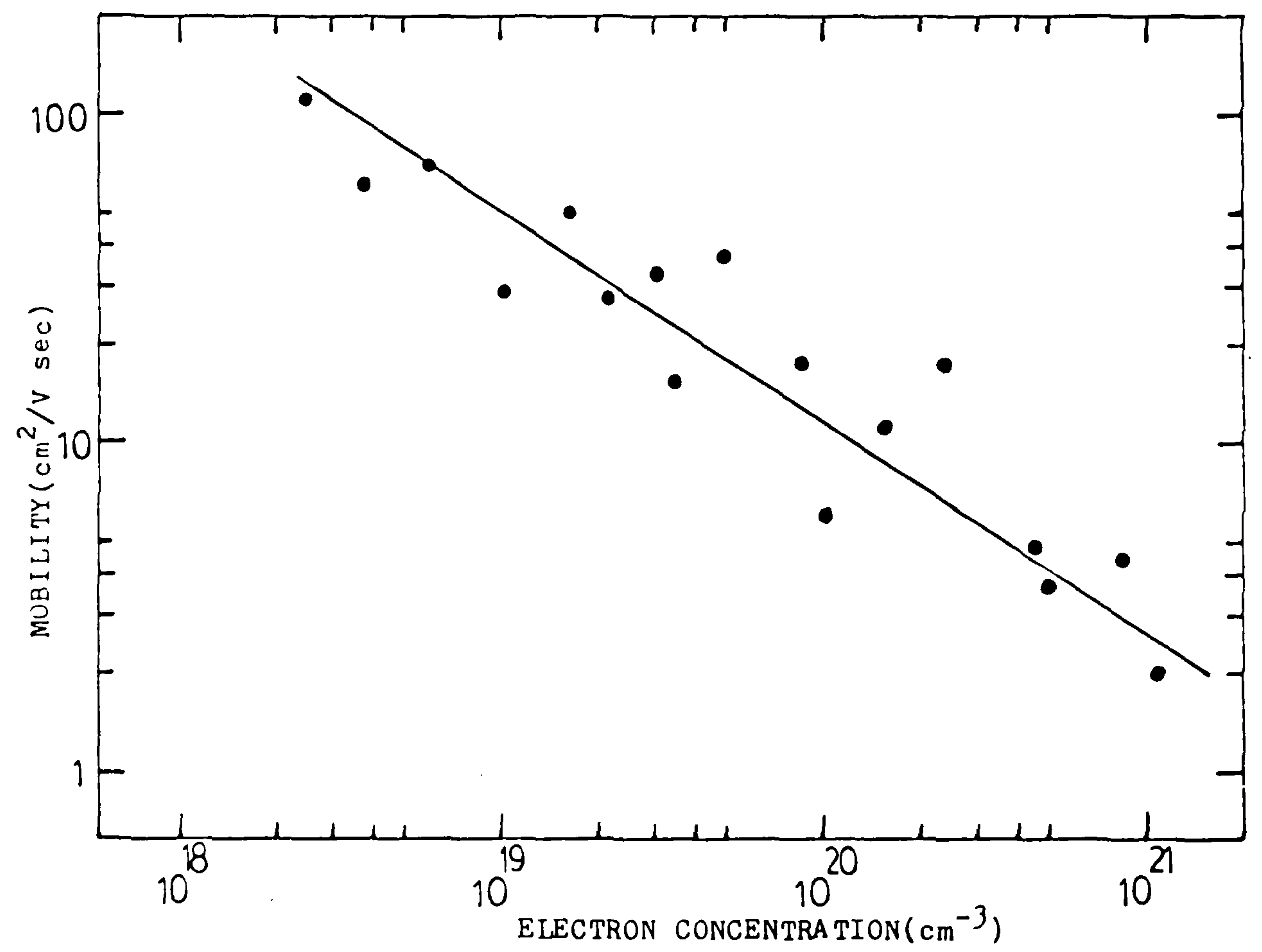

Mobility vs. electron concentration of as-grown GaN at room temperature

Fig. 2

XI. LOW TEMPERATURE PHOTOLUMINESCENCE

It has already been emphasized that all the GaN crystals grown were strongly n-type. Even after minimizing Si contamination, the GaN layers were still n-type in the 10^{18} - $10^{20}/cm^3$ carrier density range. The identity of the residual donor was not known. Because the free electron concentration in all these samples was degenerate, carrier freeze-out with decreasing temperature did not occur and transport measurements vs. temperature could not be used to elucidate the nature of this level or levels. In addition to determining the characteristics of this dominant donor, it was desired to determine the electrical behavior of a large part of the Periodic Table, both to establish the nature of shallow and deep donors in GaN as a basis for the semiconductor technology of this material, and for ascertaining if the observed residual donor could be a chemical impurity.

Low temperature (4.2°K) photoluminescence characterization seemed like an appropriate method to pursue, and our laboratory was equipped to make such measurements. We expected to see each donor and acceptor emitting at some specific wavelength. Thus, we anticipated observing each defect independently in the presence of other defects. We may expect to observe the recombination of excitons bound to neutral and to ionized donors and acceptors; we may expect to see donor-acceptor pair transitions at low temperatures and to see free-to-bound transitions at higher temperatures. Because of the high free electron density in our samples, screening should be a dominant effect, so that the observed bands should be broadened, and, perhaps, less intense than in crystals of lower carrier density. The pump we had

available was a pulsed molecular nitrogen laser, repetitively emitting high power, 10 n sec, 10^5 W peak bursts of power at 3371 Å (3.677 eV). Thus, the samples were always flooded with very high densities of electrons and holes. Under such conditions all donors and acceptors should be neutralized rapidly so that bound exciton transitions involving ionized donors or acceptors should not be seen. Luminescence from samples pumped closer to equilibrium, as might be observed from excitation by a CW low power He-Cd laser, was not obtained because we had no access to such a laser.

The lowest observed free exciton peak, from an electron at the bottom of the conduction band and a hole at the top of the highest valence band, occurs at 3.475 eV as deduced from reflectivity measurements, and, as confirmed by us, from photoluminescence, described below. Assuming a free electron mass of 0.2 m_o as deduced from the coupling of the free electron susceptibility with the reststrahlen frequency, and assuming that the hole mass is much larger, we deduce a free exciton binding energy of about 0.030 eV. This leads to a low temperature bandgap of 3.50 eV, 0.177 eV below the pump energy of the nitrogen laser.

The experimental system for obtaining the low-temperature photoluminescence data is shown in Fig. 3. The sample is immersed in liquid He and the nitrogen laser is focussed on the sample through two convex lenses and a cylindrical lens, the latter to transform the elliptical output beam into more spherical form. Filter F_1 blocks wavelengths longer than the nominal laser wavelength from reaching the sample and being reflected and detected. The emitted photoluminescence, after traversing

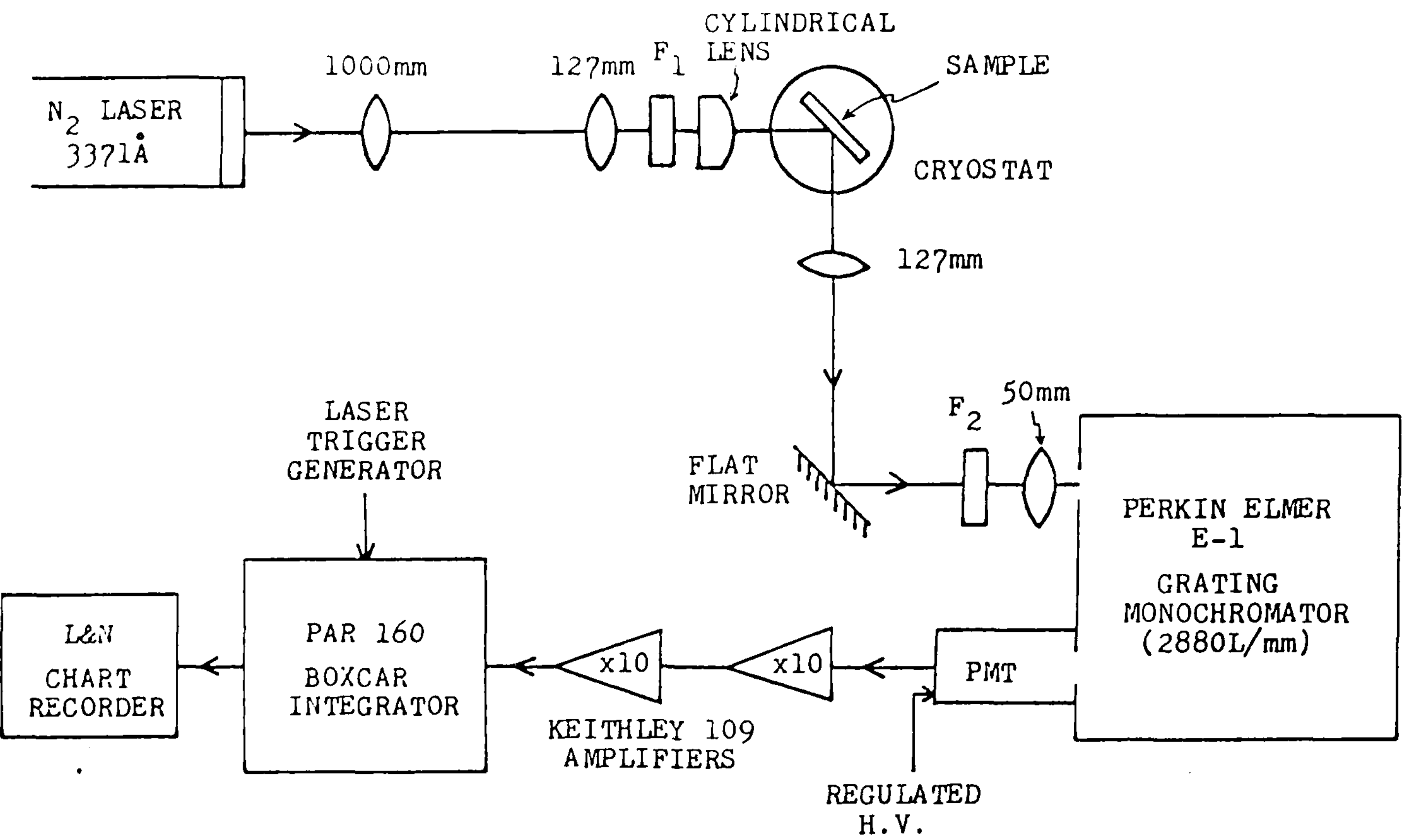

Set-up for photoluminescence measurements

Fig. 3

filter F_2, which blocks the exciting laser frequency, is focussed onto the entrance slit of a grating monochromator, whose output is detected by a UV -sensitive 1P28 photomultiplier, and, after the individual photon pulses are amplified and stretched by two fast amplifiers, they are integrated in time by a boxcar integrator (triggered by the laser signal), and recorded.

When the excitation density was very high, (when the laser focussing was very strong), emission of a broad band, well below the free exciton energy was observed. By measuring the gain spectrum in this band, we were able to show that emission was being generated by recombination within an electron-hole liquid metallic phase. From such measurements as a function of temperature, we were able to deduce the phase diagram of this e-h-liquid droplet and show that we could obtain stimulated emission from it, and, in fact, we were able to demonstrate a UV laser based on this mechanism. This is described in our Progress Report two years ago. For the remainder of the data described below, the nitrogen laser is defocussed, so that stimulated emission does not occur, and the ehl phase is not generated.

In order to begin the identification of the expected photo-luminescence emission bands at low temperatures, we start with a classification scheme, making predictions based upon the assumption that GaN is a normal semiconductor. In fact, these predictions closely parallel experimental observations for CdS, also a wide bandgap, highly ionic wurtzite semiconductor, with similar values of electron and hole masses. Here, in the presence of the very high electron densities, 10^{18} - 10^{20} cm^{-3}, we expect a good deal of line broadening. If broadening is too

great, the individual transitions would merge into one broad featureless band obscuring the contributions of the discrete states, and the method would provide us with little information, much as the electrical measurements do.

Assuming an absorption depth of about 2000 Å for the exciting laser light and a recombination time of 10^{-10} sec, we deduce that, while the laser is on and the sample output is being integrated by the spectrometer detection system, the net excitation density results in the production of 4 x 10^{27} electron-hole pairs/cm^3/sec and that this will add 10^{17} carriers/cm^3 to the steady-state carrier density. Under these conditions, the donors and acceptors most likely are kept neutral so that excitonic transitions involving neutral centers should dominate the spectra.

The predicted energies and limits to energy ranges are sketched in Fig. 4 for a temperature of 4.2°K. From the reflectivity measurements noted above, the free exciton (FE) emission band is expected to occur at 3.475 eV. From our data presented below, this line is observed at 3.4744 eV and predicted energies based upon this value of the FE are shown in parentheses in Fig. 4.

From observations of the coupled restrahlen-plasma in GaN, a value of 0.2 m_o was deduced previously for the electron mass. This is expected to be much smaller than the hole mass, so that the hole can be neglected in calculating the free exciton binding energy which becomes 0.030 eV. Added to the energy of the free exciton, this leads to a predicted bandgap of 3.505 eV at 4.2°.

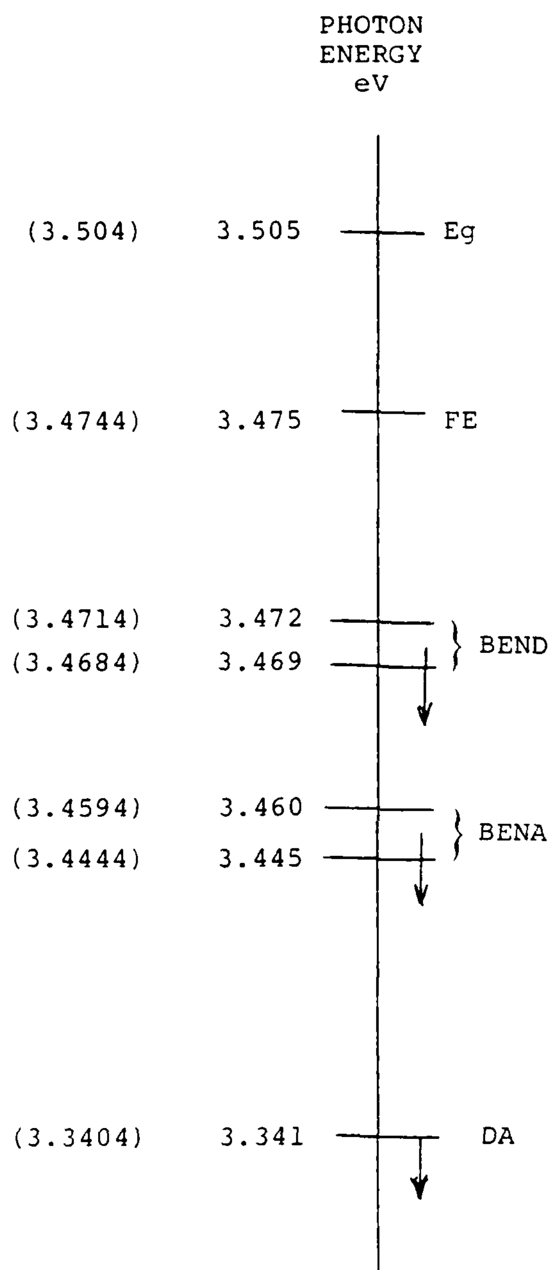

Fig. 4

With this same electron mass, and by assuming that the hole mass is about unity, it is deduced that the most shallow donor ionization energy, that determined from the effective mass approximation (EMA) is 0.030 eV and that the equivalent hydrogen-like acceptor level is 0.150 eV. All other donors and acceptors should be deeper. Excitons can bind to neutral donors or acceptors and, when the ionization energies of the donors and acceptors are not too much greater than the EMA values, the binding energies of the excitons should be linearly related to the ionization energies. This is the Haynes Rule, and the constant of proportionality, different for donors and acceptors, is the Haynes Rule constant. These constants are determined experimentally, and for all semiconductors studied they fall between 0.1 and 0.2. Thus, we predict that the smallest binding energy of an exciton to a donor in GaN will be 3-6 meV and that to an acceptor will be 15-30 meV. Subtracting these energies from that of the free exciton leads to the upper energy limits (shallowest levels) for observation of the radiative decay of an exciton bound to a neutral donor (BEND) or to a neutral acceptor (BENA). These limits are shown in Fig. 4.

At low temperatures, where both electrons and holes trapped on donors and acceptors, respectively, exhibit little thermal ionization, radiative recombination involving such trapped electron-hole pairs should be observed. This is donor-acceptor (DA) pair recombination and the energy of the emitted photon $h\nu = Eg - (E_D + E_A) + E_C$ should depend upon the separation r between the donor and the acceptor through the Coulombic energy of interaction between the two, $E_C = q^2/\varepsilon r$. Since the

donors and acceptors are randomly positioned in the crystal, r is continuous and the pair distribution is determined from statistics. The spectral distribution of the emitted radiation is determined by this distribution, by the matrix element for the transition, a function of r, and by the excitation kinetics, which depends on the method and strength of excitation, thus on the laser power and pulse shape. Hence, a broad emission band results, but its peak energy is not calculated easily. However, in most materials, and with a variety of excitation techniques, the spectral peak corresponds to a range in pair spacings, r, of between 100 and 200 Å. For GaN, this transforms to a Coulombic energy, E_C, between 16 and 8 meV. Because of the high doping density in our GaN samples, we opt for the smaller value of spacing and take our estimate for E_C as 16 meV. This term is small anyway compared to the other energies that determine the emission wavelength. In order to obtain a high energy limit for the appearance of a donor-acceptor pair band (DA), we assume the shallowest levels for both donor and acceptor, their respective hydrogenic EMA values. The peak of this highest energy DA transition is shown as a high energy limit in Fig. 4.

Since no free particles are involved in a BE transition, these lines should be very narrow, although, as noted above, they must be broadened significantly, by the high density of defects in our crystals. Because of the range of pair separations taking part in DA transitions, this band is broad inherently. The peak should shift to lower energy with time after pulse excitation and, with steady-state excitation, the emission intensity should be sublinear in excitation intensity. With increasing temperature, as the carrier trapped at the more

shallow level (usually the donor) becomes thermally ionized, the DA transition is replaced by a free-to-bound transition between a free electron and a bound hole. Here the width of the emission should reflect only the thermal distribution of the free electrons. Such a transition should behave linearly with respect to excitation intensity. In a material as highly ionic as GaN, this transition, as well as the DA transition, should be strongly coupled to the k = 0 LO phonon. Thus we expect replication of these transitions at energies of one, two, or more LO phonon energies below the phonon-less position. The LO phonon energy for GaN as determined from Raman scattering is 90 meV.

Before examining the experimental data, we note that recent calibrations of our spectrometer showed that our older calibration was not quite correct. As a result, the wavelengths given in our last two Annual Reports should be increased by 1 Å, or (at 3.5 eV) the photon energies should be reduced by 1 meV. While this correction is small in the near bandgap data range reported, 3.4 to 3.5 eV, some of the deductions which are based upon differences between these large energies are more seriously perturbed.

The free exciton, FE, is clearly detected in most of our 4.2° spectra, sometimes as a well defined peak, more often as a satellite or shoulder on another band. It occurs at 3.4744 eV, very close to the predicted value of 3.475 eV.

We begin by examining the 4.2° near-bandgap spectra from three undoped,VPE grown GaN crystals shown in Figs. 5-7. We note first, that many of these crystals exhibit bound exciton transitions well below the limiting energies determined above.

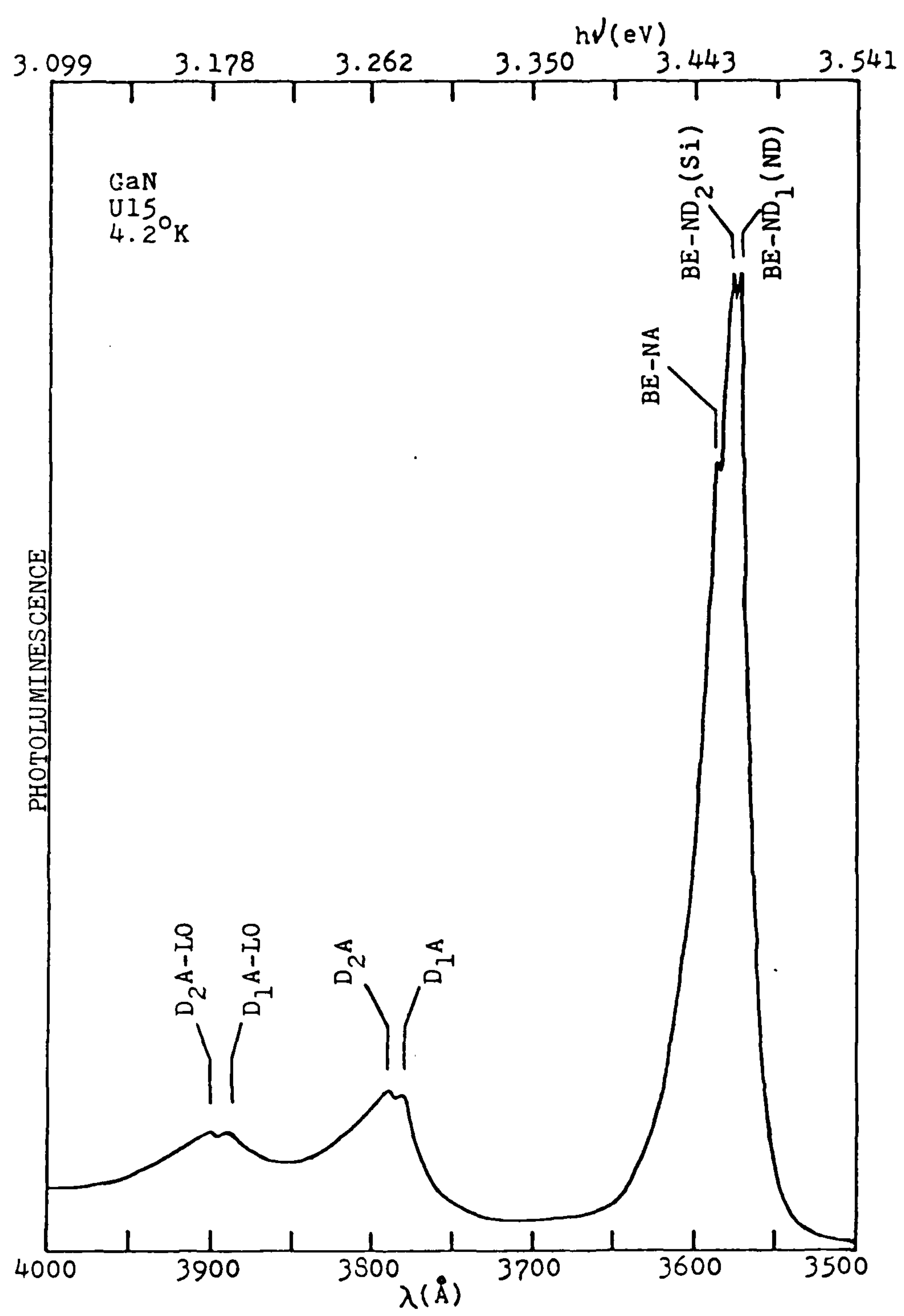

Fig. 5

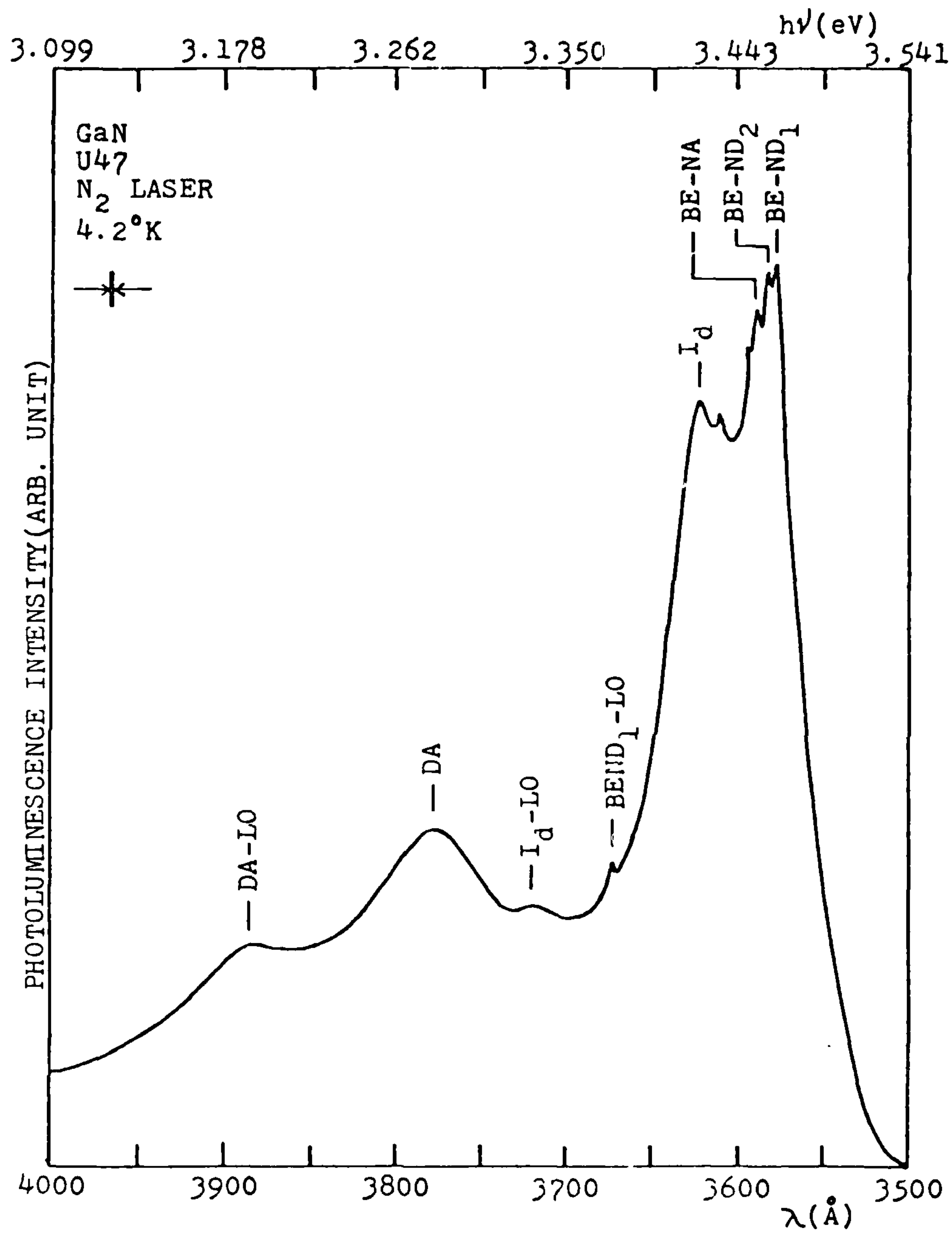

Near gap photoluminescence of GaN at 4.2°K

Fig. 6

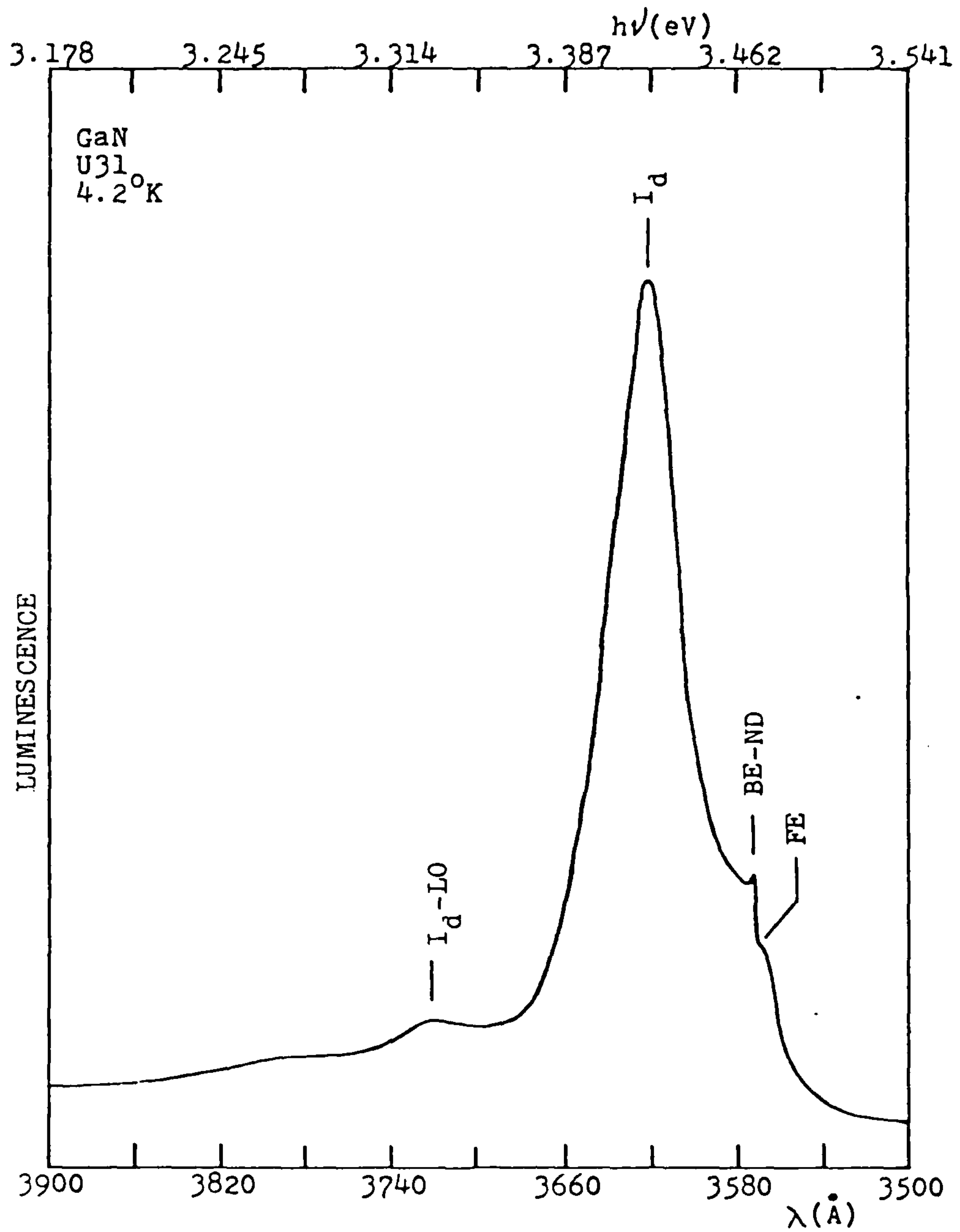

Near gap photoluminescence of GaN at 4.2°K

Fig. 7

These are broader bands due to deep donors or acceptors which are often prominent (Fig. 6) and sometimes dominate the spectrum (Fig. 7). These are labelled I_d in the figures. They are due to C and to O present as impurities, and this will be discussed later.

By comparing these spectra with the predictions of Fig. 4, as listed in Table I, it is concluded that there are bound exciton transitions with two shallow donors, and with one shallow acceptor and that two donor-acceptor bands appear each involving a shallow donor and a shallow acceptor. We will show that the higher lying (shallower) donor, ND, is the native donor which always dominates the electrical properties of our crystals, that the second (deeper donor) ND_2 is the impurity Si, that the acceptor NA is probably Zn and that the DA transitions involve the Zn as the acceptor with either the native donor or the Si donor.

Consider first, the bound exciton transitions at the shallow donors, $BEND_1$ and $BEND_2$. Corresponding to each of these peaks is a sharp but weak peak at lower energies. These are labelled as n = 2 peaks. They are barely visible in these figures; they will appear more distinctly later. Their intensity is proportional to that of the parent BE peak. Hence they must be associated with those transitions. It is assumed that they are transitions which leave the final state, that of the neutral donor, in its first excited state. This would be the first excited Rydberg state of the hydrogen-like donor. If so, then the difference in energy between the main BE peak, which leaves the donor in the n = 1 state, and the 2-electron peak, which leaves the donor in the n = 2 state, is the difference in energy

Table I

Near gap photoluminescence of GaN at $4.2^{\circ}K$

Energy position(eV)	Nature of transition
3.4744	Free exciton
3.4701	Bound exciton to neutral donor 1
3.4681	Bound exciton to neutral donor 2
3.4575	Bound exciton to neutral acceptor
3.4517	n 2 decay of exciton bound to donor 1
3.4373	n 2 decay of exciton bound to donor 2
3.4240	Bound exciton to deep level
3.3786	Bound exciton to donor 1 - LO phonon
3.3325	Bound exciton to deep level - LO phonon
3.2791	Donor-acceptor pair
3.1876	Donor-acceptor pair - LO phonon

between the n = 2 and n = 1 states of the neutral donor. We note that the ground state, the n = 1 state, has the smaller Bohr radius, and thus should exhibit much greater deviations from EMA theory (central cell corrections). We assume then that the n = 2 state is hydrogenic. Its ionization energy should then be $1/n^2$ or 1/4 that of an ideal EMA donor. This we showed above, to be 30 meV. Hence the n = 2 ionization energy is 1/4 x 30 = 7.5 meV. If this is now added to the energy between the n = 2 and n = 1 states as obtained from the difference in position between the corresponding observed BE lines, we obtain the ionization energies of the two donors. These are 25.9 meV for the native donor (ND_1) and 38.3 meV for the Si donor (ND_2).

In Fig. 5, two DA peaks are visible and the BE transitions show one acceptor (probably Zn, as already noted) and two involving these same two shallow donors. We assume the two DA transitions involve the same (and only observed) acceptor. The E_C energy of the DA transition depends only on the acceptor, since the Bohr radius of an acceptor is smaller than that of a donor (small ratio of electron-to-hole effective mass) and the concentration of the acceptor is smaller than that of the donors (n-type material). The peak positions of the two DA bands then become

$$h\nu DA_1 = Eg - (E_{D_1} + E_A) + E_C$$

$$h\nu DA_2 = Eg - (E_{D_2} + E_A) + E_C.$$

Thus $E_{D_2} - E_{D_1} = h\nu DA_1 - h\nu DA_2$ is 12.1 meV from the data of Fig. 5. From the values of E_{D_2} and E_{D_1} already determined from the BE spectra, it is 38.3 - 25.9 = 12.4 meV, in very reasonable accord.

The binding energies of excitons to these two donors as deduced above are now plotted vs. the donor ionization energy in Fig. 8. The straight line passing through these points also passes through the origin. It has a slope of 0.17, which is now the value determined for the Haynes Rule constant for donors in GaN.

These two BE peaks are observed in all samples. In the more recent, purer samples, the Si peak is suppressed, appearing only as a shoulder on the native donor BE peak. When we know Si is present as a contaminant, either in early samples, where chemical analyses showed Si contamination greater than $10^{19}/cm^3$ or in samples ion implanted with Si and annealed (see Fig. 9), the Si BE peak is present. At Si densities greater than $10^{19}/cm^3$, the Si BE peak is broadened and the neutral donor peak cannot be resolved. Here, the combined band peaks at the Si energy, whereas with little Si contamination, the remaining band peaks at the native donor position. Only with Si in the low 10^{18} cm^{-3} range, can both peaks be resolved simultaneously. Thus, from ion implantation with Si, and from chemical analyses of early crystals contaminated with Si, we establish that observed donor ND_2 is Si. To exhibit simple, almost hydrogenic donor behavior, Si must be a substitutional impurity on a Ga site. We have yet to observe any shallow acceptor, or for that matter any deep level, which could also be correlated with Si. Thus, we have no evidence that Si behaves amphoterically.

We next consider doping with group VI elements. These should be singly ionizable donors on N sites. Of these elements

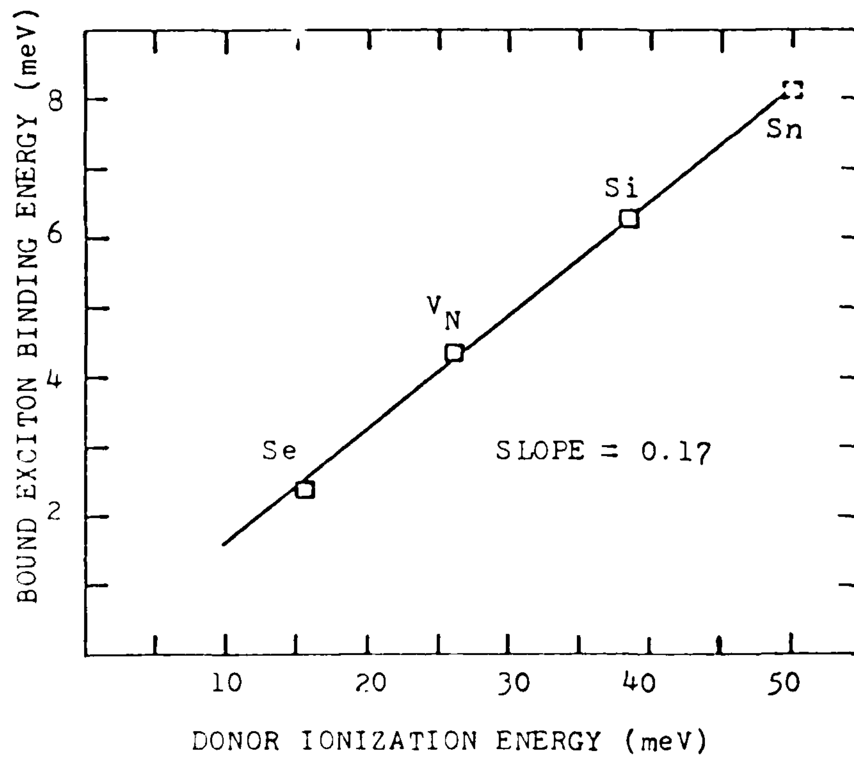

Bound exciton to neutral donor binding energy as a function of donor ionization energy determined from two-electron transition and effective mass approximation

Fig. 8

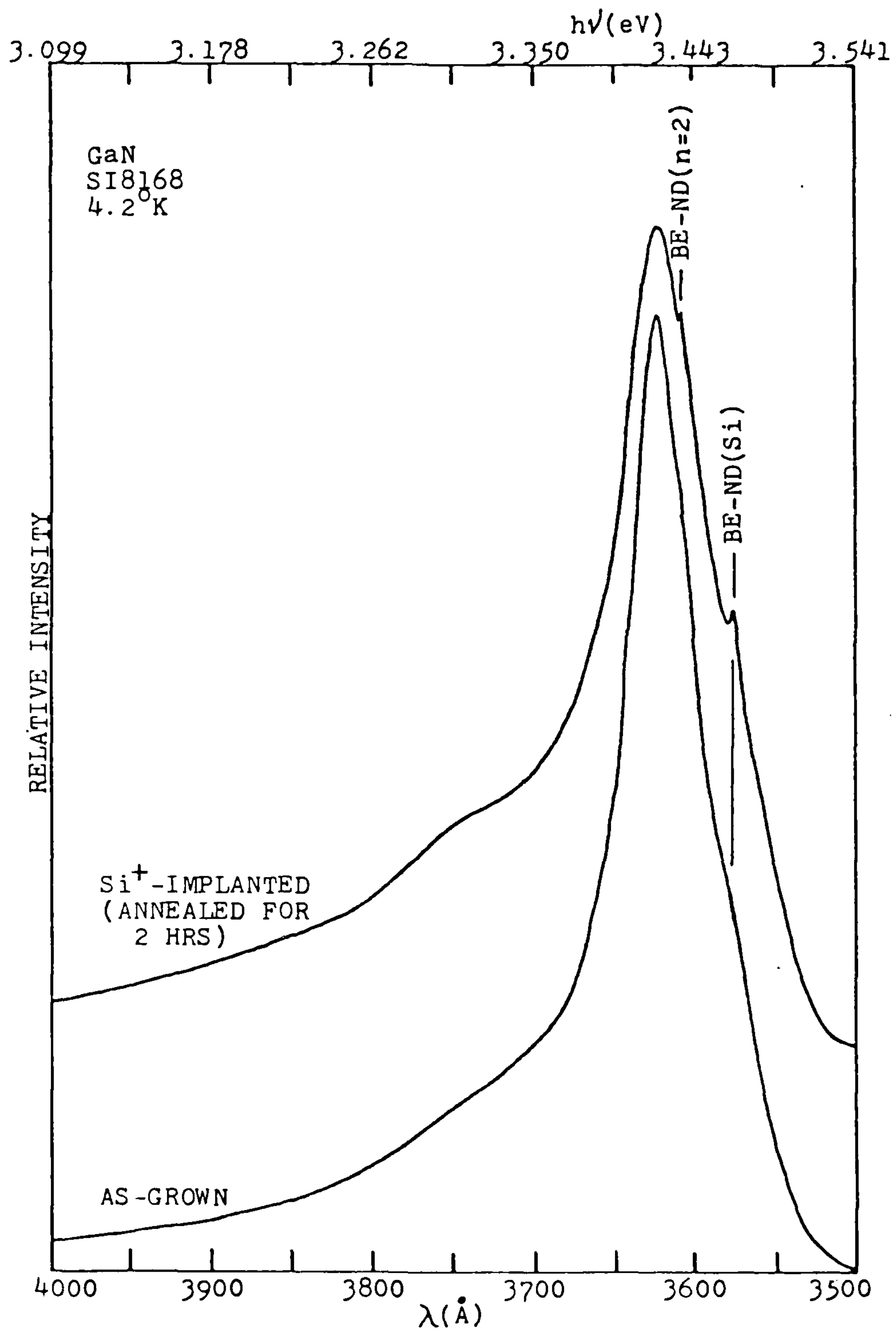

Fig. 9

(O, S, Se, Te), O and S are apparently deep levels and will be co[illegible]dered below. Te doping was not attempted. Se was implanted [illegible] one of the spectra observed is shown in Fig. 10. A bound exciton appears in the shallow neutral donor range and an n = 2 bound exciton peak also appears. These data are included in Table II and together determine a donor ionization energy of 15.3 meV. This point falls right on the donor Haynes Rule plot of Fig. 8. Se is now the most shallow donor in GaN. It is below the predicted EMA donor energy. If this Se donor is now taken as an EMA donor, we deduce an electron effective mass of 0.11 m_o, about a factor of two less than our assumed value.

Next we focus on the Group IV elements. These can be either donors or acceptors, or both. It has been shown above that Si acts primarily as a donor. C, as discussed below, has only one level and it is deep. Fig. 11 shows the spectrum of a Sn implant. It exhibits a bound exciton peak in the shallow donor range. No n = 2 bound exciton peak was resolved, but using Haynes Rule (Table II and Fig. 8) we deduce that Sn is a relatively shallow donor with an ionization energy of 50 meV. No acceptor peak is seen.

The remaining Group IV element, Ge, may indeed, be amphoteric. The behavior of Ge as an acceptor is discussed below. Here we note that whenever Ge was intentionally introduced, either during growth or by ion implantation, in addition to an acceptor bound exciton and DA band, a BE peak, virtually identical in energy to that of the shallow donor Si was introduced. It would be too much of a coincidence to suggest that Si is an impurity in the Ge sources used for doping both during growth and via ion implantation. Thus we conclude that Ge also

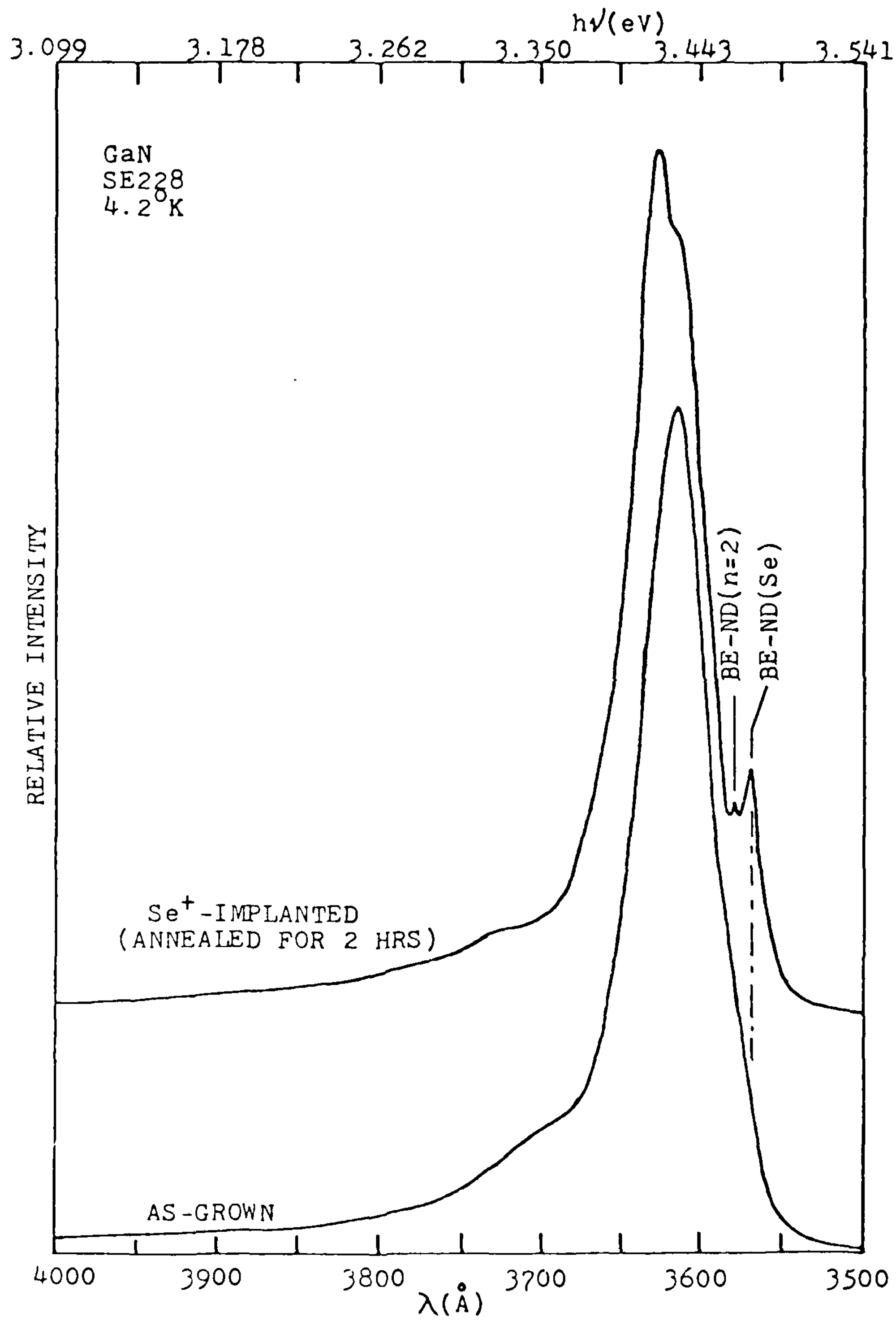

Fig. 10

Table II

Shallow donors in GaN

DONOR	BE-ND (eV)	TWO-ELECTRON TRANSITION (eV)	BOUND EXCITON BINDING ENERGY (meV)	IONIZATION ENERGY (meV)
V_N	3.47[illegible]	3.4517	4.3	25.9
Si	3.4[illegible]1	3.4373	6.3	38.3
Sn	3.4662		8.2	50.0
Se	3.4720	3.4642	2.4	15.3

Free exciton energy is at 3.4744eV at 4.2^{o}K

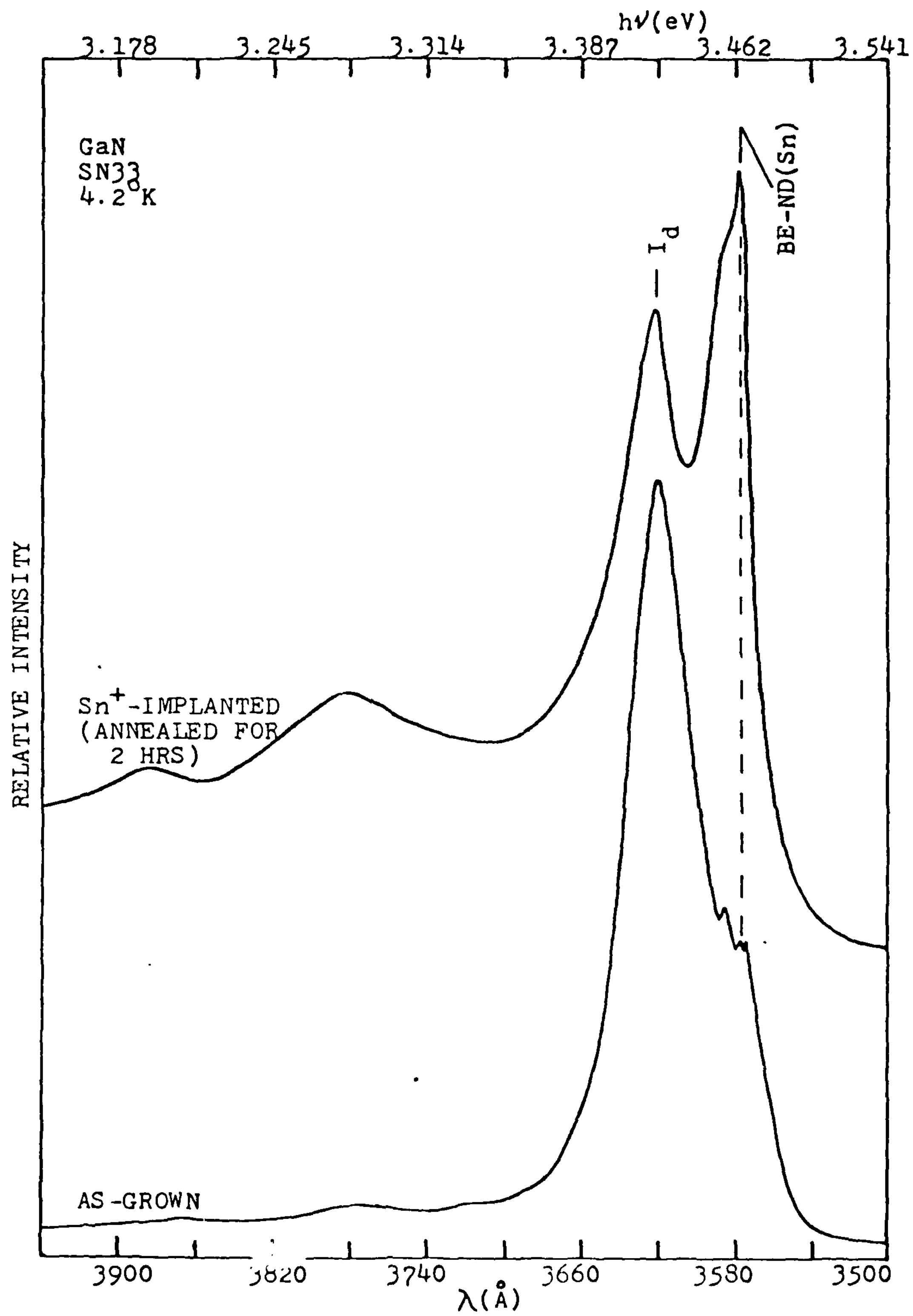

Fig. 11

behaves as a shallow donor, with an ionization energy of about 38 meV, very close to that of Si.

In summary then, the shallow donors deduced for GaN are Si, Ge, Sn, Se and the native donor defect.

We turn next to the shallow acceptors, shallow relative only to the predicted EMA value for a GaN acceptor, 150 meV. These are Cd, Zn, Be, Mg, Ge and Li studied by ion implantation, and Ge also incorporated during growth.

The 4.2° photoluminescence spectrum of a GaN sample, ion implanted with Cd is shown in Fig. 12. A bound exciton peak, clearly in the relatively shallow acceptor energy range, is evident, as well as a DA band. The DA band is identified as such, by its position, its bandwidth, and its sublinear behavior with excitation intensity (Figs. 13 and 14). A spectrum of the same crystal at 77°K is shown in Fig. 15. A band close to the DA band position now appears, but this is linear in excitation intensity (Figs. 16 and 17). It is assumed that this new band at 77° is a free-to-bound transition. A free electron in the conduction band, now thermally ionized from its shallow donor (Si or the native donor), recombines with a hole still trapped on a Cd acceptor. Assuming that the bandgap, Eg, changes little between 4.2 and 77°K, and that the mean electron thermal energy, E_t, at 77° is 6.7 meV, then, from $h\nu_{FB} = Eg + E_t - E_A$, we deduce an acceptor ionization energy for Cd of 201.4 meV. Return to the DA peak at 4.2°K. Assume that Cd is the acceptor with an energy of 201.4 meV and that the donor is the native donor (25.9 meV). Then, from the observed DA energy, $h\nu = Eg - (E_D + E_A) + E_C$, we deduce that the Coulombic energy E_C is 14 meV, corresponding to a pair separation of 113 Å. This is

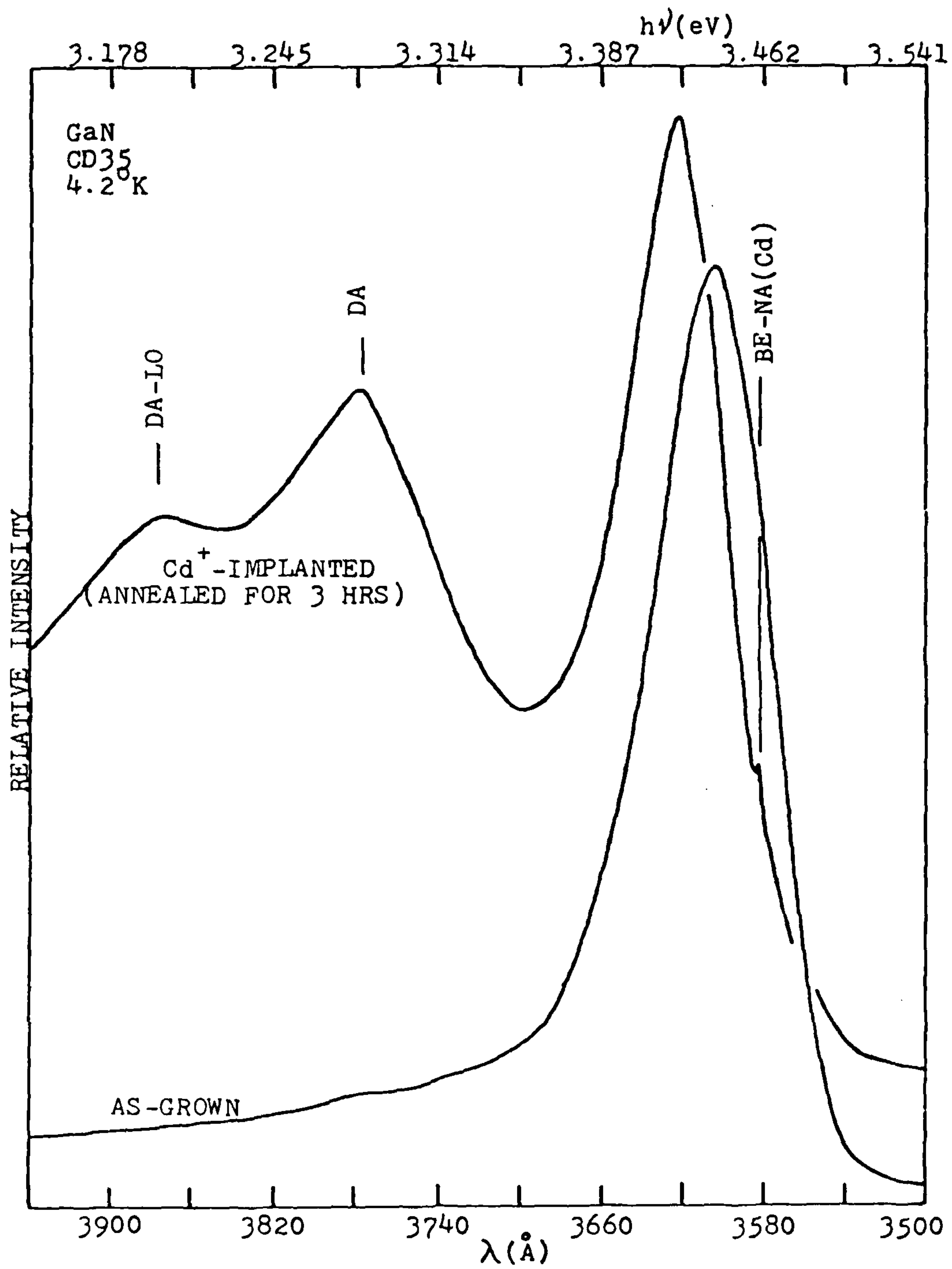

Fig. 12

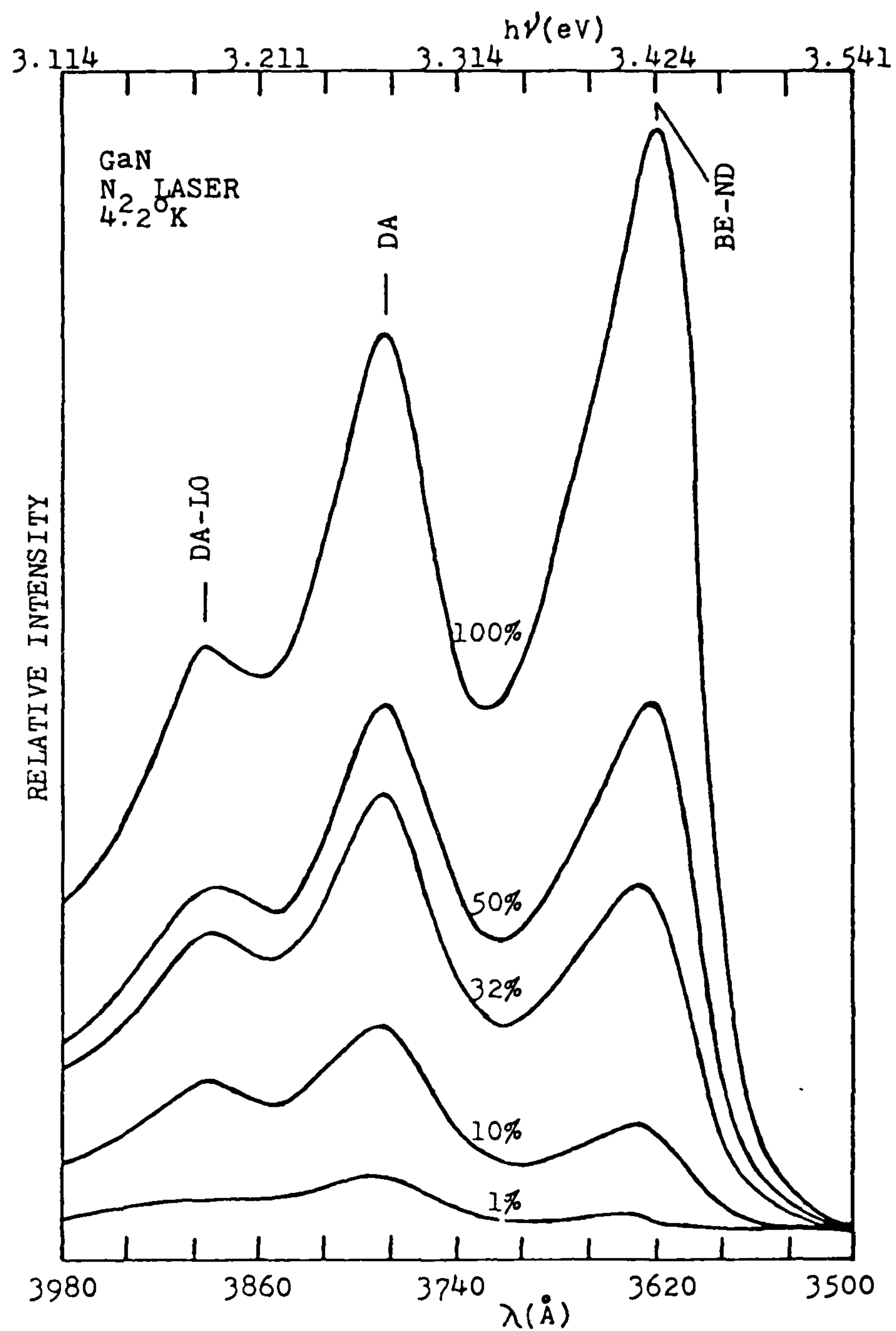

Excitation dependence of Donor-Acceptor transition in GaN at 4.2°K

Fig. 13

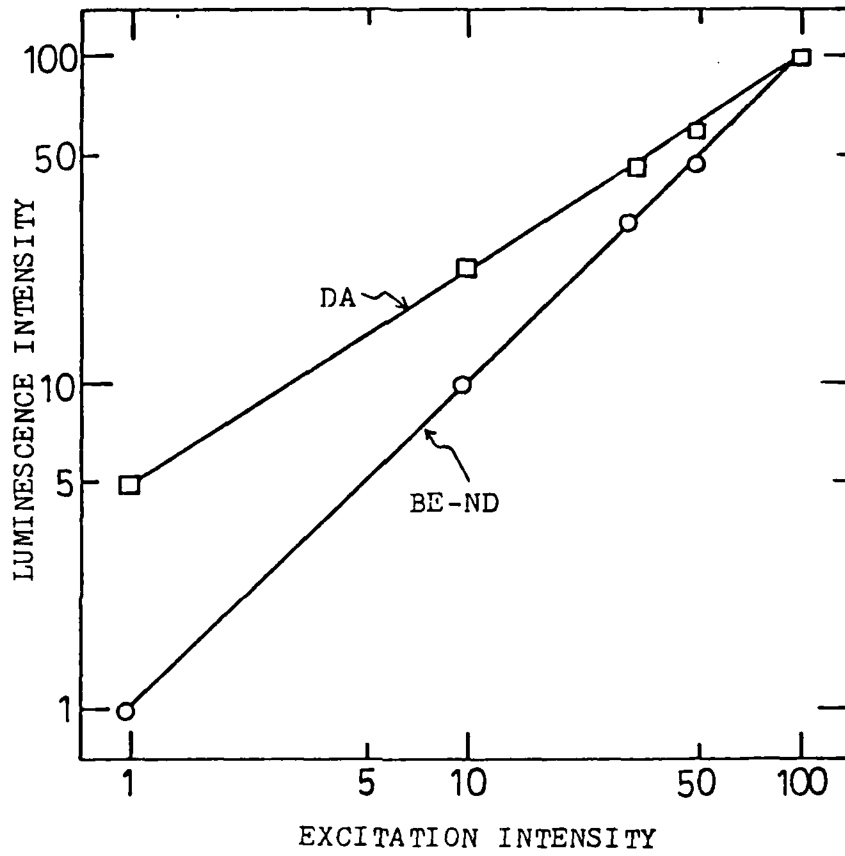

Near gap photoluminescence of GaN as a function of excitation at 4.2°K

Fig. 14

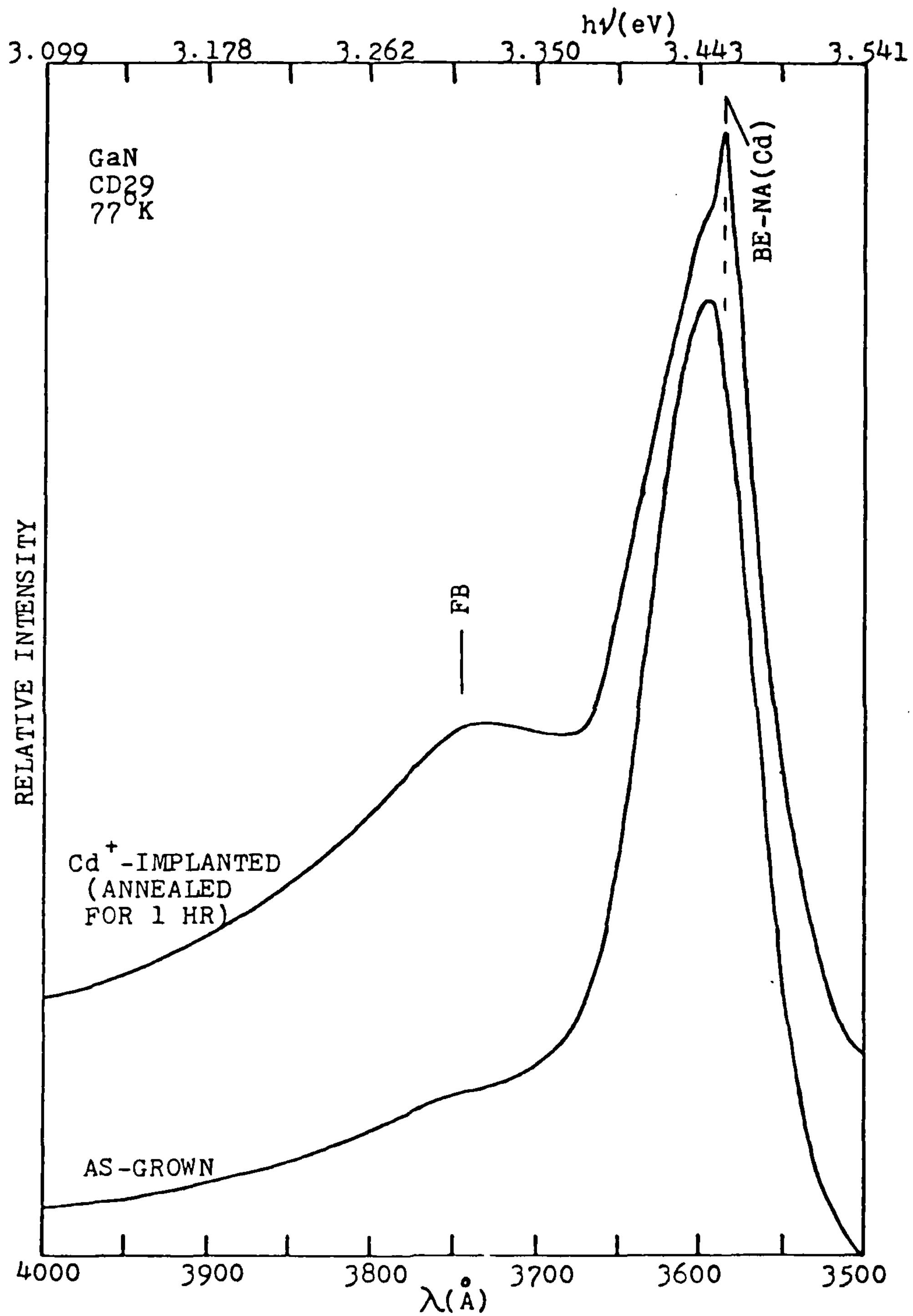

Fig. 15

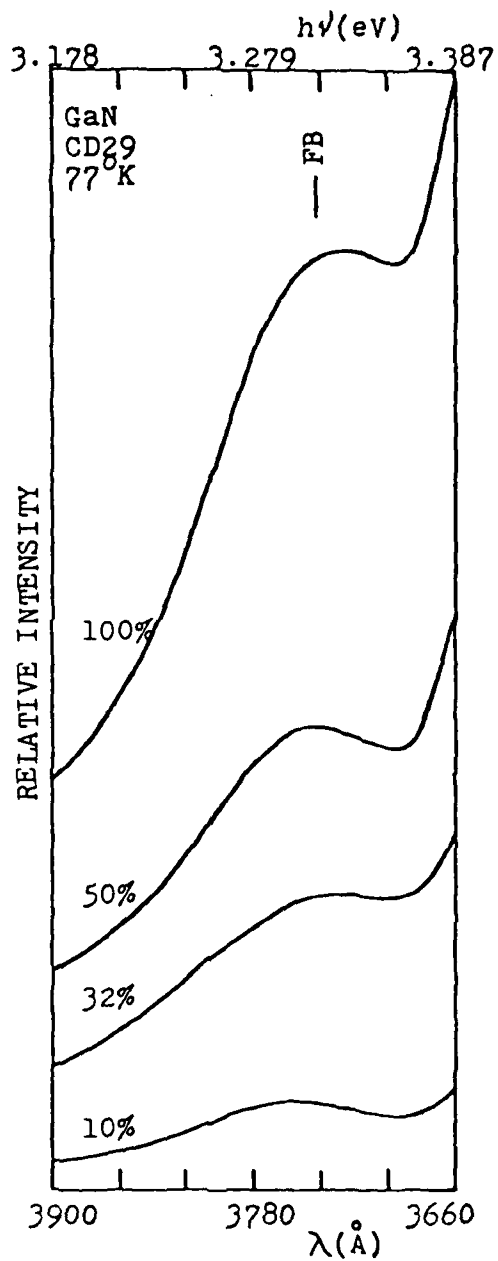

Excitation dependence of photo-luminescence of Cd ion-implanted GaN at 77°K

Fig. 16

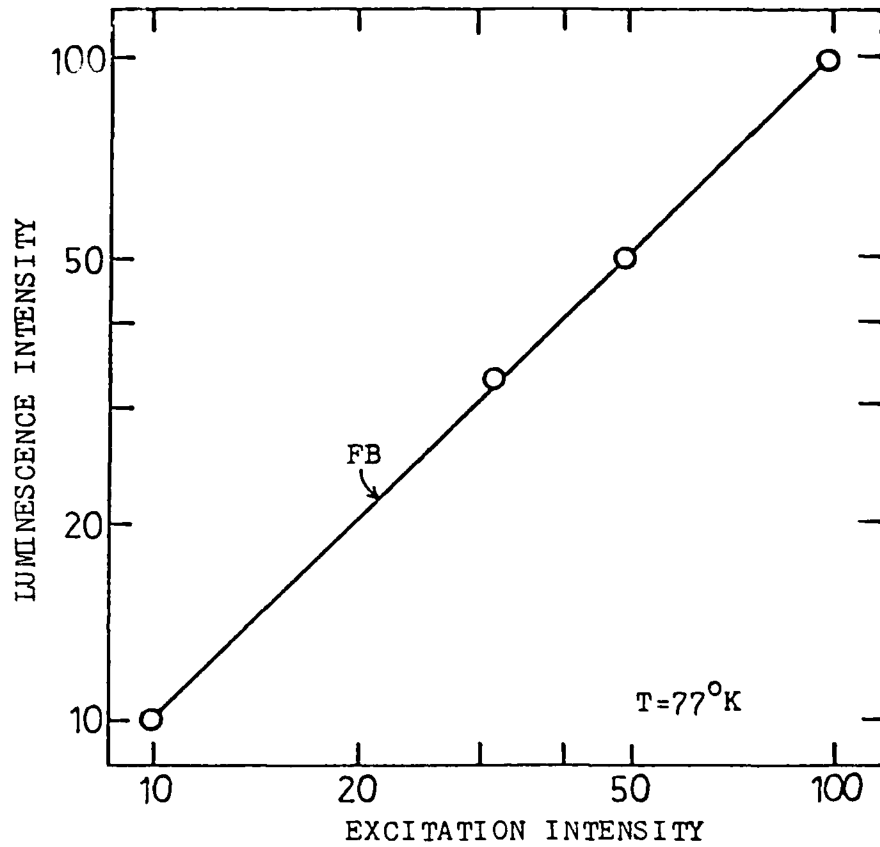

Excitation dependence of the 3.3053 eV emission, which is the transition of free electron to bound hole at Cd site

Fig. 17

identical to the Coulombic energies deduced earlier. Thus, the ionization energy of the acceptor Cd is 201.4 meV.

Next, we consider spectra due to Zn, Be, Mg, Ge and Li. These all exhibit bound exciton peaks characteristic of acceptors. These values are tabulated in Table III. For Zn, Be, Mg and Li, the spectra also exhibit the native shallow donor bound exciton line. For Ge, a peak at the Si donor position dominates. All show a broad band in the DA position which is also replicated by the LO phonon. From the position of the DA bands, and assuming that the accompanying donor is the native donor (except for Ge, where it is a donor in the Si position), and using a Coulombic energy of 14 meV, as used previously, we then deduce acceptor ionization energies for these elements as listed in Table III.

The bound exciton binding energies for these acceptors are plotted against the deduced ionization energies in Fig. 18. This results in a straight line of slope (Haynes constant) 0.11, but the curve does not pass through the origin. Note that we originally assumed (guessed) a value of unity for the hole effective mass. This predicted an EMA acceptor ionization energy of 150 meV. However, the smallest acceptor ionization energy deduced here is greater than 200 meV. Hence the hole mass must be greater than unity, about 1.3 m_o.

Li, as deduced as an acceptor, is difficult to accept. Be, Mg, Zn and Cd on Ga sites are expected to be acceptors; So is Ge on a N site. Li should enter the lattice either substitutionally on a Ga site, where it would be a doubly-ionizable, and hence, a deep acceptor, or, most probably, on an interstitial site, where it should be a donor. Let us assume for the sake

Table III

"Shallow" acceptors in GaN

ACCEPTOR	BE-NA (eV)	BOUND EXCITON BINDING ENERGY (meV)	DONOR-ACCEPTOR PEAK ENERGY (eV)	IONIZATION ENERGY (meV)
Li	3.4559	18.5	3.2722	218.7
Be	3.4581	16.3	3.2861	204.8
Mg	3.4579	16.5	3.2826	208.3
Zn	3.4575	17.0	3.2791	211.8
Cd	3.4587	15.7	3.2896	201.4
Ge	3.4584	16.0	3.2756	202.9

The donor in the D-A transition is assumed to come from the native defect (nitrogen vacancy), accept for the Ge case, where it is assumed to be due to Si.
Free exciton energy is at 3.4744 eV at $4.2^{o}K$

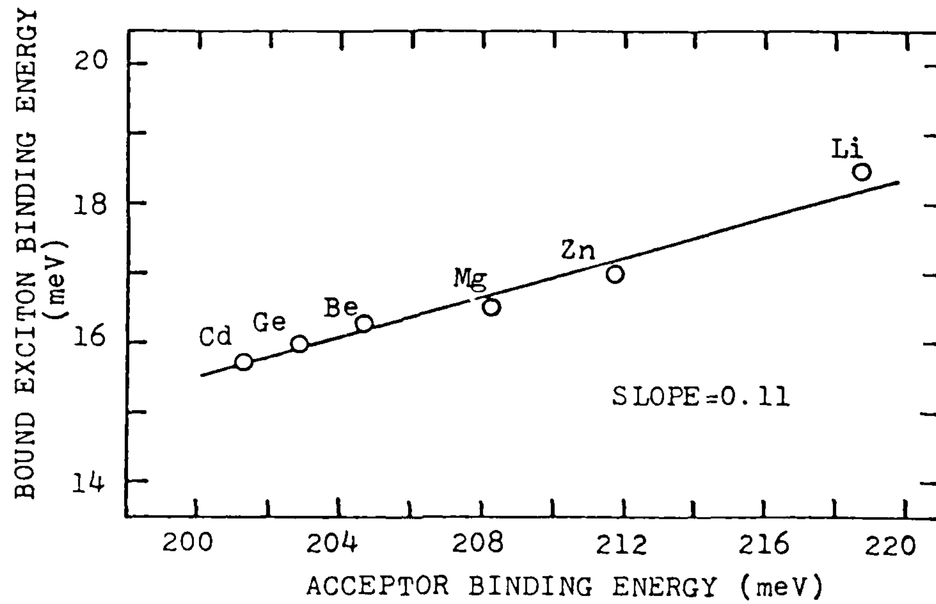

Bound exciton to neutral acceptor binding energy as a function of acceptor ionization energy determined from D-A emission

Fig. 18

of arguing that Li is a donor. Then the bound exciton peak, which occurs at low energies (overlapping the shallow acceptor regime), would yield a donor ionization energy of 0.106 eV from the donor Haynes Rule curve of Fig. 8. From the Li DA peak, using Li now as a donor, and with E_C = 14 meV, we deduce the acceptor energy as 136 meV. This is less than any acceptor energy deduced, and, in fact, it is less than our original EMA guess for acceptors. Hence we rule out this possibility. Therefore Li as observed here cannot be a donor. It must be an acceptor. Furthermore, its acceptor ionization energy, as deduced from its DA peak (assuming that the donor is the native donor, and that E_C = 14 meV), is consistent, via Haynes Rule (Fig. 18) with the position of its associated bound exciton peak.

It has been noted (see Fig. 19), that Ge-doped samples, both ion-implanted and doped during growth, exhibit a DA band, an acceptor BE line and a donor BE line at the Si donor position. We have already concluded that the donor BE line is probably due to a Ge donor. Now we focus on the acceptor level. This acceptor energy, as deduced from the DA position, here using the donor Si, or its equivalent energy, and E_C = 14 meV, as before, is 202.9 meV. The BE peak then falls right on the Haynes rule curve of Fig. 18. In Fig. 19, we also notice a weak, but narrow, peak at 3.3055 eV associated with Ge. We assume that this is an n = 2 bound exciton transition. If so, this is the only 2-electron BE transition we observe for acceptors. The difference between this energy (3.3055 eV) and the n = 1 normal BE Ge peak (3.4584 eV) should be the difference between the first excited state (n = 2) and the ground state (n = 1) of the Ge acceptor. The latter is already known (202.9 meV).

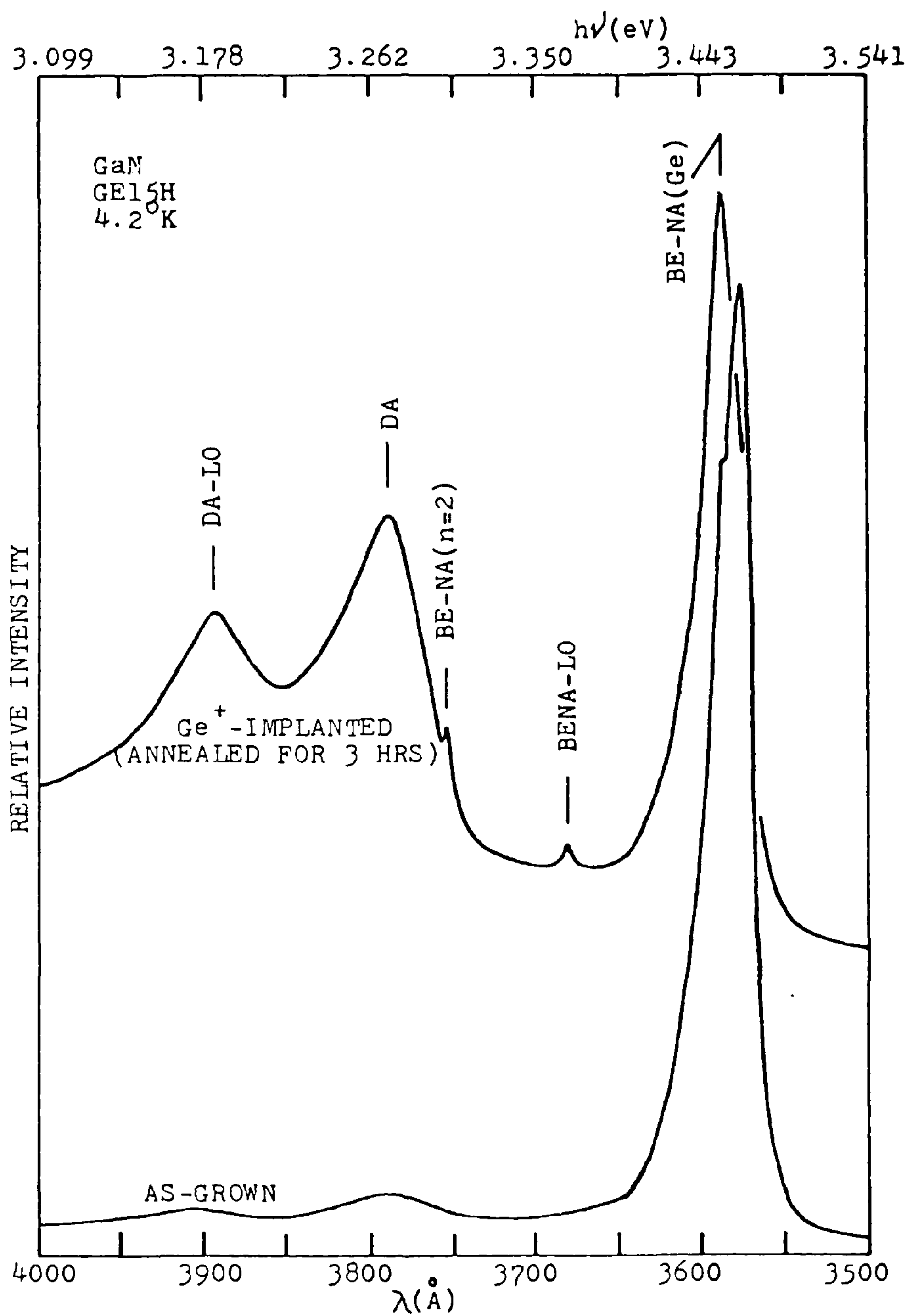

Fig. 19

Hence the first excited state is 50 meV below the ionization continuum. Assuming that this excited state is hydrogenic, agreeing with EMA theory, that is, that $E_{A(n=2)} = m_h/n^2\varepsilon^2$ 13.6 eV, we conclude that $m_h = 1.3\ m_o$. This agrees with the value we deduced above.

Referring back to Fig. 4, we note that for sharp BE peaks, there was first, a range corresponding to shallow donors and second, a range corresponding to shallow acceptors (which could also correspond to deeper donors, but only DA evidence could decide). Beyond, is a range where we would observe BE transitions involving deeper levels. Here we no longer expect the linear Haynes Rules to apply. Thus, we can no longer determine ionization energies, nor can we even deduce whether the defect is a donor or an acceptor. Note that the donor ionization energies already deduced lie between 15.3 and 38.3 meV, a range of 23 meV, and that the acceptors lie between 201.4 and 218.7 meV, a range of 17.3 meV. These cluster close to the EMA donor and acceptor energies. Now we consider impurities which generate BE peaks at energies below those corresponding to the above levels. If these are donors, their ionization energies are greater than 38 meV, if acceptors, their energies are greater than 219 meV. These peaks are tabulated in Table IV.

C was introduced both by ion implantation and during growth (from a CH_4 source). A bound exciton at 3.4165 eV is correlated with C, Fig. 20. Moreover this peak is often observed as a residual impurity band. Although C is a Group IV element, and could be amphoteric, only this one peak has ever been observed. Four-point resistivity probe measurements show no increase in resistivity as C is introduced. Hence, we guess that this peak

Table IV

Photoluminescence of deep levels in GaN at 4.2°K

Energy position (eV)	Transition
3.4527	Exciton bound to Na
3.4165	Exciton bound to C
3.3250	Exciton bound to C - LO phonon
3.4240	Exciton bound to O donor
3.4127	Exciton bound to S donor

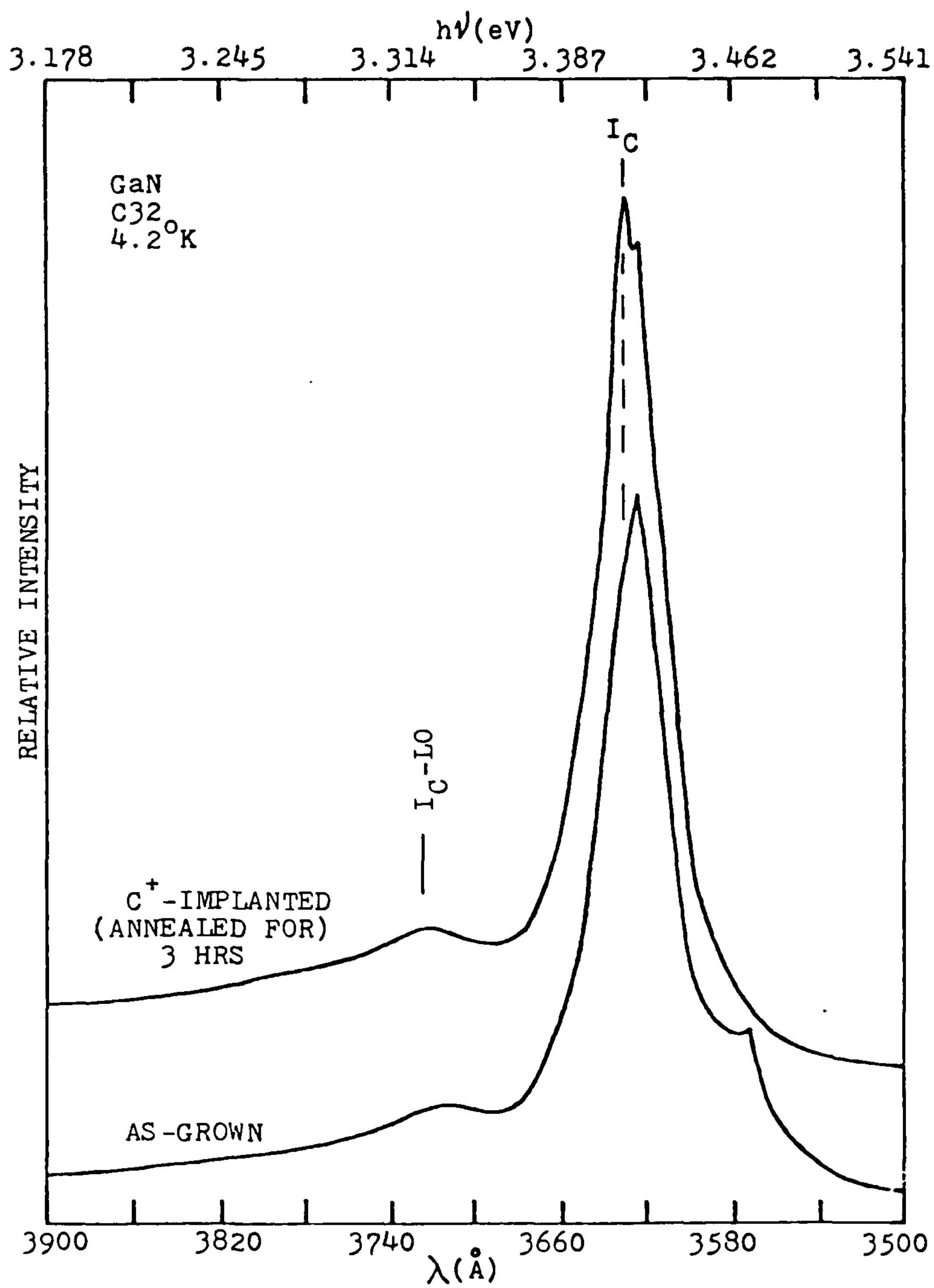

Fig. 20

is due to a deep C donor. Because we are beyond the range of validity of the Haynes Rule, we cannot estimate the ionization energy.

Another deep level is introduced by O, at 3.4240 eV. This was introduced by ion-implantation, and by adding H_2O to the growth chamber. This band also has been observed in unintentionally doped crystals. At very high doping levels, absorption into this broadened band extends into the visible range, and GaN crystals, heavily doped with O become yellow in color by transmitted light. Because O on a N site should be a donor, we suspect that O is then a deep donor in GaN.

Remember that the broad BE peaks due to O and to C are usually present in all our unintentionally doped, as-grown, GaN crystals. For both of these, we have never detected any increase in resistivity as dominated by the native shallow donor. Thus we must conclude that both C and O are deep donors.

The energies of excitons bound to deep levels are tabulated in Table IV. S, a Group VI element like Se, should be a singly ionizable donor. But, from Table IV it is clearly not shallow. Na, a suspected contaminant, should be a doubly ionizable acceptor on a Ga site, or perhaps, an interstitial defect. From ion implantation results, Table IV, it is a deep level. Its spectral position corresponds to no observed as-grown band. Hence, Na is not a significant contaminant.

From chemical analyses, we know that Al is a common impurity in GaN. However AlN and GaN are mutually soluble. Thus, Al should simply increase the bandgap and introduce no new donors or acceptors. In fact, Al, introduced by implantation, or during growth, does do exactly this. The lattice constant

increases and the bandgap increases, but no new BE or DA peaks are introduced. The observed BE and DA peaks merely shift upward as the bandgap increases.

We observe here that many of the impurities we have introduced have been studied previously by Pankove (RCA) and Jacob, Madar, et al. (France). These investigators were concerned primarily with luminescence in the visible. Their observations are presumably due to pairing of these levels with native defects giving rise to very deep radiative recombination centers active in the visible regime. Thus, their results cannot be correlated with our near bandgap, (presumably) isolated, point defect results.

Finally, we turn to the prime reason for our photoluminescence experiments, the desire to identify the shallow donor always occurring in our GaN crystals. Photoluminescence shows it as a well defined, shallow point-defect donor with an ionization energy of 25.9 meV. From Hall and resistivity data, we know that it is always present at a density of 2×10^{18} to $5 \times 10^{19}\ cm^{-3}$. Chemical analyses (emission spectrography, electron probe microanalysis, SIMS) rule out all elements in this concentration range except for the first row of the periodic table. Our doping-photoluminescence experiments have so far eliminated all elements except for H, Ga, N and the inert gases.

H was eliminated in two stages. First, H_2 is normally used as the carrier gas for the VPE growth of GaN. Replacing the H_2 with N_2 did not alter the shallow "native" donor level as observed in photoluminescence or by Hall Effect. However, NH_3 is the source of N used during growth, and this must release

H during the growth reaction. Thus the above conclusion may not be definitive. As-grown GaN samples were then implanted with protons and annealed subsequently, following our standard annealing recovery procedure (1000°C, 3 hours, in flowing NH_3). The low temperature photoluminescence spectra observed were then identical to what they were before implantation, except that all peak intensities were uniformly weaker. These results were similar to Ar ion implantations with very short anneal times. Furthermore, for the proton implanted samples, no additional luminescence in the visible was detected by eye. Thus, we conclude that H, either introduces non-radiative centers, which decrease all the luminescent peaks uniformly, or that proton bombardment introduces damage that is more difficult to anneal out than that produced by other implants. In any case, H in no way enhances the "native" donor luminescence peak. Hence, that shallow donor cannot be associated with H.

Finally, we focus in on the identity of the "native" donor. We are now in a position to assert that this shallow donor is indeed a native defect. Hall Effect and resistivity measurements show that all our GaN crystals are n-type, with an electron density between 2×10^{18} and 5×10^{19} cm^{-3}. Chemical analyses show that the only elements detected in this range are Si and Al. Elements not detectable by these analyses are H, C and O. Si is detected independently by photoluminescence. Even though it is a shallow donor, it can be minimized as a contaminant ($< 10^{18}$ cm^{-3}) by the use of high purity starting materials and by the use of an alumina liner to separate the reactant gas stream from the silica envelope of the growth apparatus. From photoluminescence, Al simply alloys

with GaN, increasing the bandgap. It is not a donor. C and O are deep levels, detected separately in photoluminescence. They are not associated with the shallow donor. H, if anything, is a non-radiative center in GaN, therefore deep. It also is not associated with the shallow level. Therefore, we are forced to conclude, that the shallow donor, which dominates the electrical properties, and which appears as the neutral donor bound exciton peak at 3.4701 eV at 4.2°K corresponding to a donor of ionization energy 25.9 meV, must be a native defect.

It was noted earlier, that our growth conditions are on the Ga-rich side of the phase diagram. Attempts at varying the Ga/NH_3 ratio did not change the native donor concentration, but rapid growth seemed to decrease it somewhat, as did growth on R-plane sapphire as opposed to basal plane sapphire. Annealing (at 1050°C) in varying NH_3 pressures had no effect.

Now we turn to implantation with N ions and with Ga ions. The photoluminescence results, after annealing at 1000°C under NH_3, are shown in Figs. 21 and 22. Although the GaN contains large amounts of C and O which produce a strong, broad, emission at lower energies, it is clear that Ga enhances the native donor bound exciton peak and that N reduces it. Thus the native donor must be associated with a N deficiency. In simplest form this is a Ga interstitial or a N vacancy. Van Vechten has shown that the energy of formation of the N vacancy is much lower than that of a Ga interstitial. Furthermore, if this were an anti-site defect, it would be either Ga on a N site or N on a Ga site. The former should be an acceptor, not a donor.

The latter should be enhanced in N, not reduced. Hence we rule out an anti-site

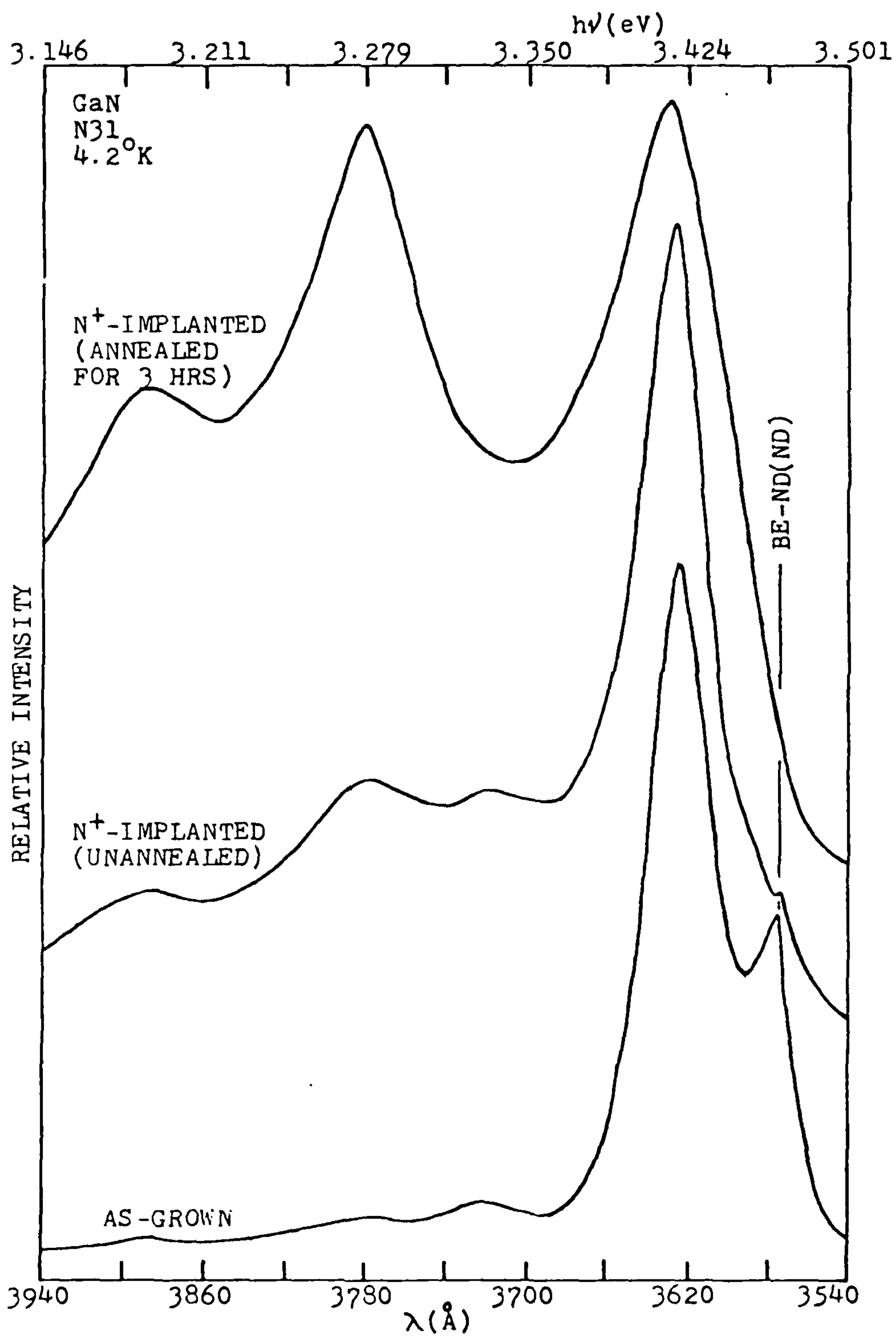

Fig. 21

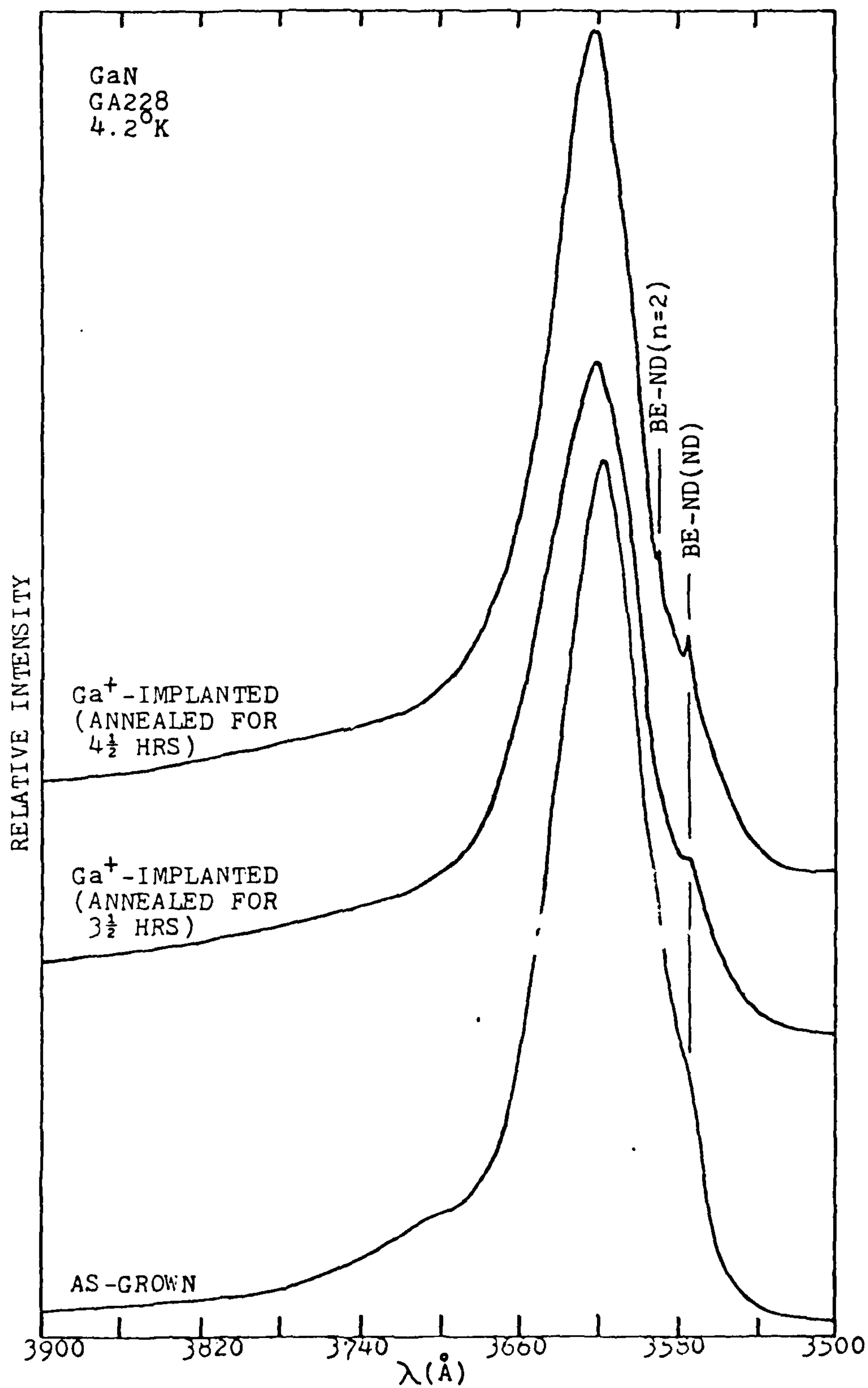

Fig. 22

defect, and conclude that the simplest model for the native donor is a N vacancy. This, of course, should be a triply-ionizable donor, although one or both of the multiply ionizable states may lie below the top of the valence band and be inaccessible.

At first glance, it may appear remarkable that a vacancy should have a very shallow, almost hydrogenic, first ionization energy. For a substitutional donor, deviations from EMA theory, leading to deeper levels, are due primarily to two features. First, in EMA theory, the wave function is automatically orthogonalized to a perfect lattice, merely adding a single positive charge to the lattice site that in reality is occupied by the donor. If the electron spends much of its time close to the donor site, i.e. if its Bohr radius is small, or if the wavefunction is peaked at the donor site, then its wavefunction should be re-orthogonalized to the core of the specific donor at the origin. This central cell correction, increasing the predicted ionization energies, seems to work well for most of the Group V donors in Si, where the corrections to EMA theory range up to about 40 meV. Second, if the donor distorts the lattice in its immediate vicinity, the constant, static dielectric constant model of the lattice must begin to break down. This effect is also enhanced if the electron Bohr radius is small, again leading to an increase in ionization energy.

We have deduced that the always-present native donor in GaN is probably a nitrogen vacancy and that its ionization energy is 25.9 meV. This energy is not much greater than the EMA value determined, 15.3 meV. This result, however, is consistent with our model for the center. First, the center

is a vacancy; thus it has no real core. Therefore, the central cell correction, re-orthogonalizing the electron wavefunction to a specific core at the center is not needed. In fact, the basic EMA model has the donor electron orthogonalized to a lattice N core at this site. But, since no atom exists here, this orthogonality condition is relaxed and the central cell correction becomes zero, or even negative. This argument would not hold if the donor were a Ga interstial, or any real chemical substitutional impurity. This is further confirmation, albeit not very strong, that the center is a vacancy. Second, we cannot believe that the lattice is not distorted around a vacancy. Here we make two observations: first, that the EMA Bohr radius (for $\varepsilon_o = 9.5$ and $m_e{}^* = 0.11\ m_o$) should be 43 Å, and second, that the ground state is possibly not an s-like state, so that the wavefunction has zero magnitude at the origin. Both these features mean that the electron spends little time close to the donor site. Hence, central cell corrections should be small. Thus, it is concluded that the low ionization energy of this defect is not inconsistent with the identification of it as a simple vacancy. In fact, after years of work, it is now believed that a S vacancy in CdS is also a shallow donor, exactly paralleling our deductions for the N vacancy in GaN.

Thus, we conclude that all our GaN crystals are dominated electrically by a native shallow donor ($2 \times 10^{18} - 5 \times 10^{19}$ cm^{-3}, ionization energy 25.9 meV) which is due to a deficiency of N. The influence of these donors could be reduced by compensation by acceptors (although at the expense of mobility) by equilibration or growth under very high N_2 pressures, and at high enough temperatures where diffusion is non-negligible, or by growth

under high N activities, as from a plasma excited in N_2.

XII. BIBLIOGRAPHY

1. M. Gershenzon, ANNUAL TECHNICAL PROGRESS REPORT, Contract N00014-67A-0269-0024, (May, 1973). AD 763413

2. M. Gershenzon, ANNUAL TECHNICAL PROGRESS REPORT, Contract N00014-67A-0269-0024, (May, 1974).

3. M. Gershenzon, ANNUAL TECHNICAL PROGRESS REPORT, Contract N00014-75C-0295, (April, 1975). AD A010215

4. M. Gershenzon, ANNUAL TECHNICAL PROGRESS REPORT, Contract N00014-75C-0295, (March, 1976).

5. M. Gershenzon, ANNUAL TECHNICAL PROGRESS REPORT, Contract N00014-75C-0295, (August, 1977). AD A045419

6. M. Gershenzon, ANNUAL TECHNICAL PROGRESS REPORT, Contract N00014-75C-0295, (September, 1978). AD A064299

7. M. Gershenzon, ANNUAL TECHNICAL PROGRESS REPORT, Contract N00014-75C-0295, (October, 1979). AD A079319

8. L. Anne and M. Gershenzon, "Defects and Morphology of Large Single Crystals of GaN Grown on Sapphire by Chemical Vapor Deposition", Electronic Materials Conference, Santa Barbara, Abstract J-2 (June, 1978).

9. M. Gershenzon and Ching-Hwa David Wang, "Shallow Donors and Acceptors in GaN from Low Temperature Near Edge Photoluminescence", Bull. Am. Phys. Soc. <u>24</u>, EL10, 336 (1979).

10. Ching-Hwa David Wang and M. Gershenzon, "EHL Recombination and Stimulated Emission in GaN", Bull. Am. Phys. Soc. <u>24</u>, E016, 343 (1979).

XIII. DISTRIBUTION LIST - FINAL REPORT
CONTRACT N00014-75-C-0295

Code 427 — 4
Office of Naval Research
Arlington, VA 22217

Naval Research Laboratory
4555 Overlook Avenue, S. W.
Washington, D. C. 20375
Code 6811 — 1
6820 — 1

Defense Documentation Center — 12
Building 5, Cameron Station
Alexandria, VA 22314

Dr. Y. S. Park — 1
AFWAL/DHR
Building 450
Wright-Patterson AFB
Ohio, 45433

ERADCOM — 1
DELET-M
Fort Monmouth, NJ 07703

Mr. Lothar Wandinger — 1
ECOM/AMSEL/TL/IJ
Fort Monmouth, NJ 07003

Dr. Harry Wieder — 1
Naval Ocean Systems Center
Code 922
271 Catalina Blvd.
San Diego, CA 92152

Dr. William Lindley — 1
MIT
Lincoln Laboratory
F124 A, P. O. Box 73
Lexington, MA 02173

Commander — 1
U. S. Army Electronics Command
V. Gelnovatch
(DRSEL-TL-IC)
Fort Monmouth, NJ 07703

Commandant — 1
Marine Corps
Scientific Advisor (Code AX)
Washington, D. C. 20380

Commander, AFAL — 1
AFWAL/AADM
Dr. Don Rees
Wright-Patterson AFB, Ohio 45433

Commander — 1
Harry Diamond Laboratories
Mr. Horst W. A. Gerlach
2800 Powder Mill Road
Adelphia, MD 20783

Advisory Group on Electron Devices — 1
201 Varick Street, 9th Floor
New York, NY 10014

Professor L. Eastman — 1
Phillips Hall
Cornell University
Ithaca, NY 14853

Professor Hauser and Littlejohn — 1
Department of Electrical Engr.
North Carolina State University
Raleigh, NC 27607

Professor Rosenbaum & Wolfe — 1
Semiconductor Research Laboratory
Washington University
St. Louis, MO 63130

Professor Robert Davis — 1
North Carolina State Uni.
P. O. Box 5995
Raleigh, NC 27607

END
DATE
FILMED
6-81
DTIC